QUANTIFYING ATMOSPHERIC FALLOUT OF FUKUSHIMA-DERIVED RADIOACTIVE ISOTOPES IN THE HAWAIIAN ISLANDS

A THESIS SUBMITTED TO
THE GEOLOGY AND GEOPHYSICS DEPARTMENT

MAY 2016

By
Trista McKenzie

Thesis Advisor

Henrietta Dulai

I certify that I have read this thesis and that, in my opinion, it is satisfactory in scope and quality.

THESIS ADVISOR

Henrietta Dulai
Department of Geology and Geophysics

ACKNOWLEDGEMENTS

This thesis would not be possible without the collaboration, help, and support from several parties. First and foremost, I would like to thank my thesis advisor, Dr. Henrietta Dulai, for her guidance, encouragement, time, and patience throughout this project. This project would not have been possible without her expertise.

I would also like to thank Jan Kamenik, Petra Kamenikova, La Noa O Pono A. Keahinuuanu, Carl Berg, and Lynx Gallagher for their work on the mushroom collection and analysis.

I am also grateful to Dr. Mike Garcia for his time and assistance to teach me how to crush the basalt samples.

Additionally, I would like to thank my friend, Leslie Chatham-Toy for her company and assistance in collecting soil and basalt samples on the Big Island.

Finally, I would like to thank my husband, Warren McKenzie, for his encouragement and support throughout this process.

Trista McKenzie

ABSTRACT

On March 11, 2011, several reactors at the Fukushima Dai-ichi Nuclear Power Plant suffered damage and released the radioisotopes iodine-131, cesium-134, and cesium-137 into the atmosphere. A week later, these isotopes were detected in aerosols over the state of Hawaiʻi and in milk samples analyzed from the island of Hawaiʻi. Because the detected levels were significantly below levels of health concern, the state did not attempt to quantify the deposition of these nuclides on the islands. This study estimated the magnitude of atmospheric fallout of cesium and iodine, and examined the patterns of cesium wet deposition with precipitation observed in March 2011. Mushroom and soil samples were collected along precipitation gradients on Oʻahu and the island of Hawaiʻi and analyzed for cesium isotopes using gamma spectrometry. Fukushima-derived fallout was differentiated from historic nuclear weapons testing fallout by the presence of ^{134}Cs, which has a shorter half-life of 2.06 years and the fact that ^{134}Cs and ^{137}Cs were released from the severed power plant nearly in parity. We found that Fukushima-derived cesium was present in both mushrooms and soil and the soil inventories ranged 20-600 Bq/m^2 for ^{134}Cs and 130-4,600 Bq/m^2 for ^{131}I. Additionally, we found that Fukushima-derived cesium inventories in soils were correlated with precipitation gradients. This research confirmed and quantified the presence of Fukushima-derived fallout in Hawaiʻi, however the activities detected were an order of magnitude lower than fallout associated with the nuclear weapons testing in the Pacific.

TABLE OF CONTENTS

LIST OF TABLES

LIST OF FIGURES

LIST OF ABBREVIATIONS AND SYMBOLS

Abbreviation	Definition
INES	International Nuclear Event Scale
EPA	Environmental Protection Agency
FPP/FDNPP	Fukushima Power Plant/ Fukushima Dai-ichi Nuclear Power Plant
FDA	Food and Drug Administration
NISA	Nuclear and Industrial Safety Agency
PBq	Peta Bequrel = 10^{15}
IAEA	International Atomic Energy Agency
DOE	Department of Energy
ROI	Radionuclide of Interest
HPGe	High Purity Germanium
SRM	Standard Reference Material
CPM	Counts Per Minute
CL	Critical Level
TF	Transfer Factor

Symbol	Definition
Y	Gamma yield of peak
A	Activity of ROI isotope
C	Net count rate per minute
$T_{1/2}$	Radioactive half-life
ε	Relative efficiency
E_{γ}	Radioactive decay energy

CHAPTER 1. INTRODUCTION

On March 11, 2011, the Fukushima Dai-ichi Power Plant experienced significant damage from a tsunami that followed the 9.0 magnitude Tohoku earthquake. The three reactors that were running during the earthquake were immediately put on an emergency shutdown (Thakur et al., 2013) and emergency generators managed the cooling systems. Approximately fifty minutes later, a subsequent tsunami hit the power plant. While the Fukushima Dai-ichi Power Plant had a ten-meter high sea wall, it was not enough to prevent the incoming tsunami of estimated height of thirteen to fifteen meters (Pararas-Carayannis, 2014). The seawater proceeded to flood the basement that housed the emergency generators, disabling them. This resulted in the loss of cooling capability, overheating of the reactors, and the partial meltdown and damage of three of the six nuclear reactors.

Starting on March 12, 2011, significant amounts of radioactive isotopes were released into the environment via atmospheric routes. Between March 14 and March 17, 2011, the severed power plant released the most radionuclides with a peak on March 15 (Thakur et al., 2013). The Fukushima Power Plant accident was classified as a Level 7 on the International Nuclear Event Scale (INES), indicating a major nuclear accident because of the high initial amount of radionuclides released into the environment (Thakur et al., 2013).

As a result of the Fukushima Dai-ichi Nuclear disaster, radioactive isotopes including ^{131}I, ^{134}Cs, and ^{137}Cs were released into the atmosphere. In addition to these radioisotopes, other volatile fission products were released into the atmosphere as well. The majority of the radioactive aerosol plume from Fukushima then proceeded west in the direction of the Pacific Ocean. Between March 19 and March 24, 2011, the Environmental Protection Agency's (EPA) RadNet air filters detected these isotopes on the islands of Oʻahu, Kauaʻi, and Hawaiʻi along with other locations in the Pacific (Environmental Protection Agency, 2011; Figure 1.1). It should be noted that the activity levels of the radionuclides detected were very low and not remotely near action levels determined by the EPA.

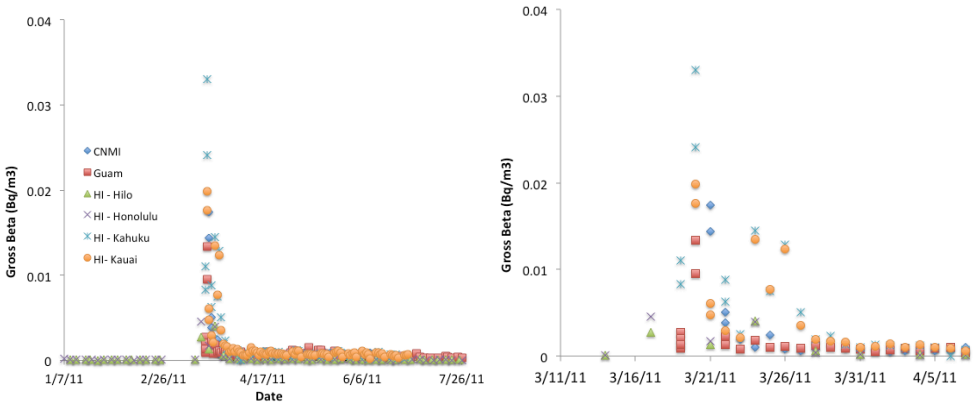

Figure 1.1: Gross beta radiation detected in the air in 2011 before, during, and after the FPP accident by EPA's RadNet system (Environmental Protection Agency, 2011). Gross beta includes all beta radiation emanating radionuclides; it is not specific to iodine or cesium. The peak shows that the majority of the plume passed above Hawaiʻi between March 19 and March 26, which is when most of the deposition was expected to happen.

On March 22, 2011, the EPA published a press release informing that Fukushima-derived radioisotopes had been detected in air masses over the western United States. EPA's RadNet air samplers had detected ^{137}Cs, ^{134}Cs

^{132}Te, ^{132}I, and ^{131}I. All activity concentrations were hundreds of thousands to millions of times below the level of concern (Environmental Protection Agency, 2011). Additionally, ^{131}I was detected in milk samples on the island of Hawaiʻi, but these levels were deemed 5000 times lower than the level of concern outlined by the Food and Drug Administration (Department of Health, 2011).

The EPA's RadNet air filters and cartridges, which were analyzed for individual isotopes, detected the maximum activity for the radionuclides ^{137}Cs, ^{134}Cs, and ^{131}I for air around the islands of Oʻahu and Kauaʻi. For Kauaʻi, the maximum values were 2.8 ± 0.2 x 10^{-3} Bq m^{-3}, 2.9 ± 0.2 x 10^{-3} Bq m^{-3}, and 4.0 ± 0.3 x 10^{-2} Bq m^{-3} for ^{137}Cs, ^{134}Cs, and ^{131}I respectively. For Oʻahu, the maximum values detected were 4.4 ± 0.6 x 10^{-3} Bq m^{-3} (^{137}Cs), 3.4 ± 0.3 x 10^{-3} Bq m^{-3} (^{134}Cs), and 3.0 ± 0.2 x 10^{-2} Bq m^{-3} (^{131}I). The average particulate ^{131}I to particulate ^{137}Cs activity ratio detected by the EPA's RadNet air filters from March 20 until April 1, 2011 for Kauaʻi was 5.3 ± 3.4. For Oʻahu, the average particulate ^{131}I to ^{137}Cs activity ratio was 7.3 ± 2.8. For the same dates, the average non-particulate ^{131}I detected by EPA's RadNet air cartridges to particulate ^{137}Cs activity ratio for Kauaʻi was 6.1 ± 4.1. For Oʻahu, it was 13.0 ± 7.2. Furthermore, the average ^{131}I activity found in precipitation from April 4 to April 13, 2011 was measured at 8.03 ± 3.4 x 10^{-2} Bq/m^3. Both ^{137}Cs and ^{134}Cs were below the minimum detection level in precipitation for these dates.

^{134}Cs and ^{137}Cs readily attach to particles in the atmosphere (Thakur et al., 2013). and are therefore relatively easy to quantify on air filters that capture suspended particles. The Nuclear and Industrial Safety Agency (NISA) of Japan initially estimated that 15 PBq (Petabecquerel: = 10^{15} Becquerel) of ^{137}Cs was released into the atmosphere. Several months after the nuclear disaster, this result was lowered by NISA to 11 PBq of ^{137}Cs (Thakur et al., 2013). Additionally, ^{134}Cs and ^{137}Cs derived from Fukushima were released at a near one to one uniform ratio (Buesseler et al., 2011).

^{131}I, unlike cesium isotopes, is not uniformly distributed between the gaseous phase and that attached to particles and much of the iodine stays in the form of a gas not associated with particulates or aerosols (Thakur et al., 2013). This makes ^{131}I very difficult to accurately quantify. In addition to air filters, charcoal cartridges are used to capture gaseous iodine. The International Atomic Energy Agency (IAEA) has created an accepted means of converting ^{134}Cs and ^{137}Cs activity concentrations to reach an ^{131}I equivalent. NISA used this method to derive an initial ^{131}I atmospheric release of 770 PBq. This result was later recalculated to a much lower value of 130 PBq (Thakur et al., 2013).

Atmospheric fallout is primarily deposited by means of precipitation (Wetherbee et al., 2012). Since cesium and iodine isotopes were detected in air and precipitation it is fair to assume that the Hawaiian Islands experienced wet deposition of these nuclides. Indeed, iodine and cesium were detected in milk samples in Hawaiʻi. Moreover, it was suggested by a

health study published earlier (Mangano and Sherman, 2013) that Fukushima-derived ^{131}I in the atmosphere caused a notable increase in congenital hypothyroidism amongst newborn babies born in the western United States and the state of Hawaiʻi during the three-month period after the meltdown. This is inconsistent with the EPA's data that showed that radioactivity concentrations in air and milk were well below a level that would concern human health. This is an example how conflicting information may mislead the concerned public in the absence of actual estimated data on the amount of radionuclides deposited after the accident. Therefore, the objective of this research is to investigate the levels of deposited radionuclides.

The Hawaiian Islands experience unique rain patterns due to the prevailing trade wind patterns and thus one hypothesis is that wet deposition was driven by rain distribution in March 2011. Indeed, it has been previously determined by measuring soil samples in Hawaiʻi that there is a positive linear relationship between precipitation and cesium fallout from nuclear weapons tests (Cox & Fankhauser, 1984). Atmospheric nuclear weapons' testing was most prevalent from 1945-1963. During this time an estimated 950 PBq of cesium was released (UNESCO, 2000) that left a positive fingerprint on the islands. This study investigates how Fukushima releases compare to those inputs. During atmospheric releases the radionuclides are not homogeneously distributed in the atmosphere, in addition their fallout is driven by meteorological conditions, especially

precipitation. The concentrations are generally higher in mountainous areas or oceanic environments where precipitation is largest (Cox & Fankhauser, 1984). Because precipitation rates on the Hawaiian Islands are higher on the windward side of the islands this is where higher radionuclide concentrations are anticipated as well. Cox & Fankhauser demonstrated that after the nuclear weapons tests fallout there was a predictable pattern in ^{137}Cs activities in soil and rock samples that suggested that the higher rainfall deposited higher activities of cesium.

Building on Cox & Fankhauser's conclusions and the RADNET data that showed the presence of Fukushima-derived radionuclides in the atmosphere above the islands in March 2011, the purpose of this study was to quantify the atmospheric fallout derived from Fukushima in the state of Hawaiʻi in order to test the hypothesis that 1) the atmospheric fallout in the Hawaiian Islands was present and 2) wet deposition was the major driver of radionuclide deposition and there is a positive correlation between rain and deposited amounts of cesium. Because the newly deposited cesium levels were expected to be low and suspected to be near detection limits for soil samples we took advantage of bioaccumulation of cesium in organisms and analyzed mushroom samples to confirm the presence of fallout. Mushrooms have been shown to be good indicators of the presence or absence of cesium fallout in Europe (Duff et al., 2008) and Asia (Nakashima, et al., 2015). For our study mushrooms were collected along precipitation gradients as locational indicators for wet cesium deposition. After confirming the

presence of fallout, soil samples were collected in the same locations as the mushrooms. From there, average mushroom cesium uptake to precipitation ratio for the Hawaiian Islands was derived. The soil measurements and the information of radiocesium to ^{131}I ratios in the air as detected by the EPA and DOE were then used to estimate the amount of ^{131}I that has been deposited via precipitation.

1.1 Mushrooms as bioindicators of cesium contamination

Certain species of mushroom have previously been determined to be good bioindicators of radionuclide deposition from studies following the Chernobyl nuclear disaster (Duff et al., 2008). Mushroom species that have gills, pores, or spines and have stalks have been shown to have a stronger affinity for radiocesium and are less dependent on growing in soil that encourages radiocesium uptake (Duff et al., 2008). Mushrooms with these characteristics typically have a higher mycelium concentration and have a longer average lifespan (Castro et al., 2012). Additionally, it has been shown that the greatest amount of cesium accumulates in the cap of the mushroom (Oolbekkink, 1989).

In addition to differences between mushroom species, certain soil characteristics have been shown to positively influence radiocesium uptake by mushrooms. The bioavailability of radiocesium in soil is strongly correlated to the concentration of clays, specifically exchangeable potassium (Seeger, 1978). Stable cesium concentration in the soil has shown to be

inversely related to radiocesium uptake (Oolbekkink, 1989). Additionally, it has been shown that soils with a pH of 6 or greater will allow for maximum radiocesium uptake. Using this information, one can assume that clays or alkaline soils should have higher bioavailable radiocesium concentrations than an acidic or organic soil. It has also been shown that mushrooms growing in decaying wood uptake significantly less radiocesium than all other substrates (Oolbekkink, 1989). Moreover, given the large number of factors that influence cesium uptake by mushrooms, the transfer factor (TF), which is the ratio of radiocesium activity concentrations (Bq/kg) in mushroom to the radiocesium concentration per soil area (Bq/m^2) may differ by up to 200 times (Kaduka et al., 2006).

Following the Fukushima nuclear disaster, studies have been conducted on mushrooms within close proximity to the FDNPP. One study found that 81.2% of wild mushrooms collected within 30 km of the FDNPP contained over 100 Bq/kg of radiocesium and 36.4% of those contained over 1000 Bq/kg (Nakashima, et al., 2015).

1.2. Radiocesium behavior in soils

Experiments following the Fukushima Dai-ichi nuclear disaster have shown that a majority of the ^{137}Cs and ^{131}I deposited in soil tends to remain in the top five centimeters of the vertical soil profile (Tanaka et al., 2012). The authors suggest this is because both ^{137}Cs and ^{131}I have a strong affinity for soil compounds. In the case of ^{137}Cs, the authors demonstrate that ^{137}Cs

tends to bind with clay minerals in the soil and greater than 87% of Fukushima derived ^{137}Cs was found in the top five centimeters of soil. Similarly, the authors demonstrate that ^{131}I tends to bind with humic materials, and more than 76% of Fukushima derived iodine was found in the top five centimeters of soil (Tanaka et al., 2012). Further studies on the migration of pre-Fukushima ^{137}Cs in soils in forests near the FDNNP have shown a very slow downward migration averaging at 0.46 mm/year with Fukushima-derived ^{137}Cs having negligible downward displacement. (Teramage, et al., 2016). This is consistent with experiments conducted after Chernobyl, which demonstrated that ^{137}Cs deposited in the topsoil layer is adsorbed into that layer and can be bioavailable for long periods of time (Filipovic-Vincekovic et al., 1991).

Other evidence speaks for low cesium migration in soils and sediments. The presence of ^{137}Cs from nuclear fallout from the 1960's is used in sedimentation rate studies (Ritchie et al., 1990). In these studies sediment cores are collected and analyzed for excess ^{210}Pb and the presence of ^{137}Cs. The layer containing ^{137}Cs is assumed to have formed in the 1960's. This application further supports the general assumption that cesium is stabilized in soils and sediments for many decades. Therefore we assume that nuclear weapons testing fallout can still be accurately captured in the topsoil. Furthermore, we assume that we can confidently use our soil samples collected in the top 5 cm of soil in 2015 to estimate the fallout from 2011.

1.3. Wet deposition of radionuclides in soils

While this study focused on ^{137}Cs and ^{131}I deposition there are other natural radionuclides, ^{210}Pb and ^{7}Be, which are well correlated with wet deposition. This study therefore also evaluates ^{210}Pb to track long-term wet deposition rates in order to correlate with pre-Fukushima cesium deposition. Additionally this study also evaluates ^{7}Be in order to track the last few months of wet deposition. While neither of these nuclides can help quantifying cesium fallout, their presence and trends can help evaluate wet deposition and rain correlations and further validate our assumptions about cesium fallout.

CHAPTER 2. METHODS

2.1 Sample collection

Mushrooms were collected at few selected sites along precipitation gradients on Kaua‘i, O‘ahu, and Hawai‘i between 2012-2013. Where possible, mushroom species that have shown to preferentially uptake cesium (i.e., are gilled and/or have stalks (Duff et al., 2008), for example the genus Boletus) were collected. At least 100 g of wet weight of mushroom was collected, cleaned of soil and plant debris, and placed in a clean plastic bag. Mycologists (Professor Brian Perry and Lynx Gallagher, UH Hilo and Dr. Carl Berg, Surfrider, Kaua‘i) identified the genera and/or species of the collected mushrooms where possible. Otherwise, mushrooms of unidentified species were collected. The geographic location and time and date of sample collection were recorded.

Soil samples on O‘ahu and Hawai‘i were collected between 2015 and 2016 at the same locations as the mushrooms. In addition, surface soil was collected approximately at the same locations as reported by Cox & Fankhauser on O‘ahu and Hawai‘i. At each site of sample collection, approximately 5 cm topsoil was collected and any factors that could have altered deposition, such as canopy cover, were noted. Approximately 250 grams of soil were collected into clean plastic bags that were sealed and transported to the laboratory for further processing.

2.2 Sample Preparation for Gamma Spectroscopy

Mushroom samples were initially allowed to air dry to constant mass in a fume hood with forced air circulation. The samples were then weighed to record dry mass. After this step the samples were ashed in a ceramic crucible for over a total period of 10 hours at 200°C for the first hour, 350°C for the second hour, and 450°C for the remaining eight hours. Samples were then homogenized by a pestle and transferred to a 30-cm^3 tin crucible for analysis by gamma spectroscopy.

Each soil sample was sieved through a 4.0 mm opening sieve, cleaned of plant debris, and oven-dried for 72 hours at 60°C. To homogenize the soil, each sample was ground with a pestle prior to being placed in the crucible. Basalt samples were physically crushed and sieved through a 1.0 mm opening sieve.

80 mL of each soil and basalt sample were transferred to a 120 mL polypropylene crucible for analysis by gamma spectroscopy. Mushroom, soil, and basalt samples were stored for at least 21 days prior to analysis by gamma spectroscopy to ensure equilibrium between ^{226}Ra and ^{222}Rn.

2.3 Sample Analysis by Gamma Spectroscopy

Measurements by gamma spectroscopy were executed with an Ortec coaxial HPGe detector, which has a relative efficiency of 43% and a resolution of 1.76 keV based off the 1.33 MeV gamma line for ^{60}Co. Gamma-spectra were analyzed using Hypermet-PC V5.01 software (Révay et al., 2001). Samples on average were counted until there were 1000 counts in the primary ^{137}Cs peak, or about 96 hours. Samples that presented a primary ^{134}Cs peak were counted for one week.

Background activity levels were determined by running an empty crucible of the same geometry. Gamma energy in keV and peak intensities for the primary radionuclides of interest (ROI) are listed in Table 2.3.1. Secondary ROI, which were evaluated only for internal check for example for equilibrium in the uranium decay chain and in case of ^{226}Ra to calculate excess ^{210}Pb, are listed in Table 2.3.2.

Table 2.3.1: Gamma energy (keV) and peak intensities (%) for the primary radionuclides of interest.

ROI	**Gamma Energy (keV)**	**Intensity (%)**
^{134}Cs	604.0	97.6
^{137}Cs	661.7	85.2

Table 2.3.2: Secondary ROI and their respective gamma energies (keV) and peak intensities (%).

ROI	Gamma Energy (keV)	Intensity (%)
^{210}Pb	46.4	4.25
^{234}Th	63.1	3.70
^{235}U	185.7	57.20
^{212}Pb	238.6	43.60
^{214}Pb	351.9	37.17
^{7}Be	477.7	10.44
^{228}Ac	911.2	25.8
^{214}Bi	609.3	15.3
^{40}K	1460.8	10.7

2.4. Sample Analysis – Physical Characteristics

Some physical characteristics of the soil samples were analyzed, including bulk density, particle density, and porosity. The particle density of the soil was determined by adding 30 g of previously dried and ground soil to 70 mL of water in a 100 mL graduated cylinder. Equation 1 was used to determine the particle density.

$$Particle\ Density = \frac{mass\ of\ dried\ soil\ added\ (g)}{volume\ of\ water\ displaced\ (mL)} \qquad \text{Eq. 1}$$

Bulk density of the soil was determined by adding dried and ground soil in 20 cm^3 increments to a 100 mL graduated cylinder. After 80 cm^3 of compacted soil was added to the graduated cylinder, it was weighed. Bulk

density was determined by comparing the mass of soil added to the volume of soil added according to Equation 2.

$$Bulk\ Density = \frac{mass\ of\ dried\ soil\ added\ (g)}{volume\ of\ soil\ added\ (mL)} \qquad \text{Eq. 2}$$

Percent porosity of soils was then calculated by taking the measurements of particle density and bulk density in Equation 3.

$$Percent\ Porosity\ = \left(1 - \frac{Bulk\ Density}{Particle\ Density}\right) \times 100\% \qquad \text{Eq.3}$$

2.5. Rainfall Data Collection

Rainfall amounts in March 2011 were found for each sample location using the Hawai‘i Rainfall Atlas (Giambelluca, et al., 2013). The rainfall atlas provides data for geographic location defined by the user based on its latitude and longitude. Rainfall measurements for March 2011 were found for each location of sample collection, as previously marked by GPS. Rainfall in mm was then plotted against radiocesium activities in mushrooms and soil in order to assess a potential correlation between the two.

For ^{7}Be analysis of soils, the National Weather Service's rain gauge data was used because the Hawai'i Rainfall Atlas has not yet published data for 2015 and ^{7}Be deposition is recent given the shorter half-life of ^{7}Be ($t_{1/2}$ = 53.24 days). For each sample, the rainfall data from the closest station to the sample was found for the month in which the sample was collected and was used and compared in a similar manner as above.

2.6. Data analysis

To determine relative efficiency (ε) of the HPGe detector, a sediment standard reference material (SRM) IEAE-385 was packed in the same geometry as the measured soil samples. The standard was then counted for 84000 seconds on the detector and the spectrum was evaluated for each radionuclide of interest (ROI). The detector efficiency (ε) was calculated using Equation 4, where C is the net count rate per minute (CPM), Y is the gamma yield of the individual gamma-peak, m is the dry mass of the sample in kilograms, and A is the activity of the isotope of ROI in Bq/kg:

$$\varepsilon = \frac{C_{net}}{Y \times m_{SRM} \times A} \qquad \text{Eq. 4}$$

The SRM was only certified for certain radionuclides, which did not include ^{7}Be and ^{134}Cs. Because there is a unique relationship for each detector between peak energy and detection efficiency, efficiencies of ROI not present in the SRM could be calculated. For ^{7}Be and ^{134}Cs, efficiencies were derived by finding the second-order polynomial equation which best fit

the ROI present in the SRM as shown in Figure 2.6.1 and the efficiency of the appropriate radionuclide decay energy in kEV (E_γ) was found by interpolation.

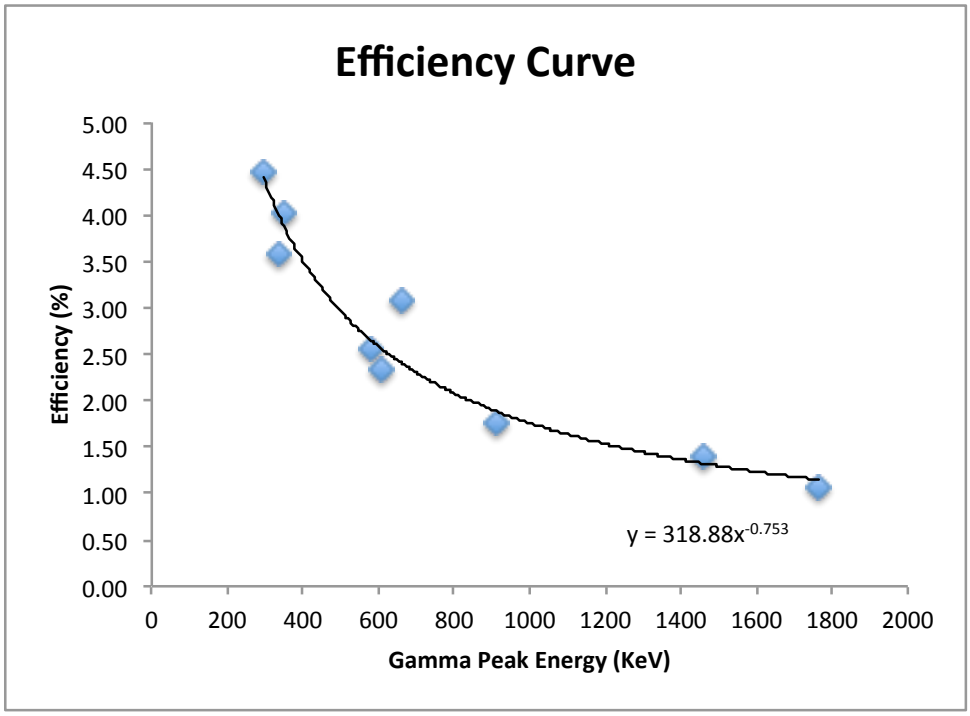

Figure 2.6.1. Derived efficiency curve.

Critical level (CL) concentrations for ROI in each sample were calculated using the following equation, which accounts for uncertainties originating from detection efficiency, sample mass, and background counting rate and time. Equation 5 gives the equation used to determine CL concentrations where N_B is the number of counts in the blank, t_s is the amount of time the sample was counted in seconds, t_B is the amount of time the blank was counted in seconds, m_{sample} is the mass of the sample, Y is the gamma yield of the individual peak, and ε is the detector efficiency. Where

measurements were below the critical limits of our method as determined by the CL, results are reported as "<CL".

$$CL = \frac{2.33 \times \sqrt[2]{(N_B} \times \frac{t_S}{t_B} \times (1+\frac{t_S}{t_B}))}{m_{sample} \times t_s \times Y \times \varepsilon} \qquad \text{Eq. 5}$$

The results were decay corrected to two different dates; March 20, 2011, the date that the highest atmospheric radioactivity was detected over Hawai'i for the cesium isotopes, and the date of sample collection for ^{7}Be and ^{210}Pb, using Equation 6 where α represents the activity for the ROI in Bq/kg, $T_{1/2}$ is the half life of the ROI in years:

$$A = A_t e^{\frac{\ln(2)}{T_{1/2}} t} \qquad \text{Eq. 6}$$

Where t is the time between sample collection and analysis. The Fukushima-derived, newly deposited cesium activities were estimated by assuming a 1:1 ^{137}Cs and ^{134}Cs activity ratio at time of release in March 2011. Old, pre-Fukushima activities were then calculated by subtracting ^{134}Cs decay corrected to March 2011, which should equal to ^{137}Cs at the time of sampling (90% of ^{137}Cs still present), from total ^{137}Cs. New and old fractions of ^{137}Cs were then compared to evaluate Fukushima deposition to the cesium previously deposited from the nuclear weapons testing (Cox & Fankhauser, 1984).

In addition to cesium fallout, ^{131}I fallout was inferred using the average particulate ^{131}I to ^{137}Cs activity ratio (7.3 ± 2.8) as detected by the EPA's RADNET system in Hawai'i and our measured ^{134}Cs fallout.

Excess ^{210}Pb was also calculated in order to assess wet deposition trends in soil samples on the investigated transects. It was calculated by first averaging the activities of ^{214}Pb ($t_{1/2}$ = 26.8 minutes) and ^{214}Bi ($t_{1/2}$ = 19.9 minutes) to find the activity of ^{226}Ra. Because the daughter products of ^{226}Ra have comparatively shorter half-lives (^{214}Pb $t_{1/2}$ = 19.7 minutes and ^{214}Bi $t_{1/2}$ = 26.9 minutes), they are in secular equilibrium.

Excess ^{210}Pb activity was then calculated as shown in Equation 7, where all activities are in Bq/kg.

$$A_{Pb210excess} = A_{Pb210} - A_{Ra226} \qquad \text{Eq. 7}$$

CHAPTER 3. RESULTS

Mushroom, soil, and basalt samples were collected between 2012 and 2016. Sampling locations are shown in Figures 3.1.1 and 3.1.2.

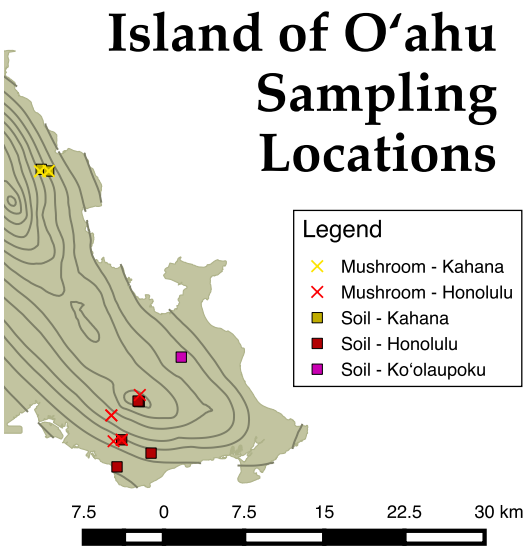

Figure 3.1.1. Island of O'ahu mushroom and soil sampling locations. Soil samples are denoted by a square and mushroom samples are denoted by an x. Contours represent March 2011 precipitation gradients with a contour interval of 25mm and represent a range of 25 to 600mm of rainfall (Giambelluca, et al., 2013).

Figure 3.1.2. Island of Hawai'i mushroom, soil, and basalt sampling locations. Soil samples are denoted by a square, mushroom samples are denoted by an x, and basalt samples are denoted by +. Contours represent March 2011 precipitation gradients with a contour interval of 25mm and represent a range of 25 to 900 mm of rainfall (Giambelluca, et al., 2013).

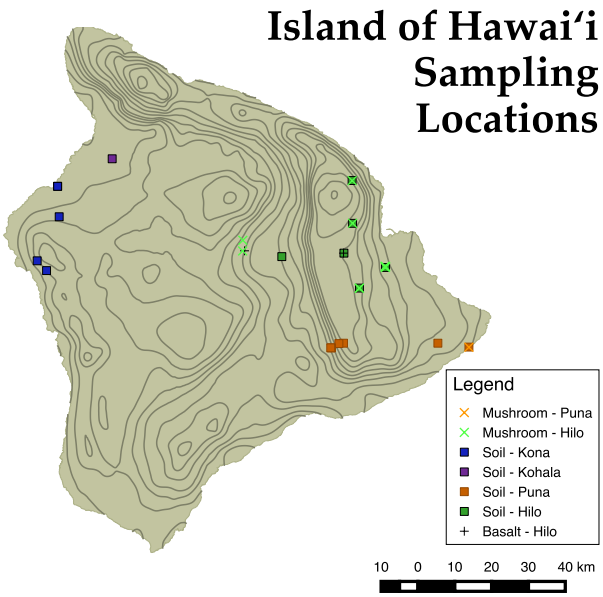

Soil samples were collected on Oʻahu and the island of Hawaiʻi in 2015 and 2016. Soil sampling locations, collection dates, and their wet and dry weights are tabulated in Table 3.1.1.

Table 3.1.1. Locations of soil sample collection, the date of collection, and pre and post drying weight (g).

ID	Island	Sample Location	Date Collected	Lat Lon	Wet Wt (g)	Dry Wt (g)
1	Oʻahu	Kahana Valley	4/5/15	21.54, -157.89	564 ± 28.2	365 ± 18.3
2	Oʻahu	Mānoa Falls	3/8/15	21.33, -157.80	457 ± 22.9	278 ± 13.9
3	Oʻahu	Kahana Dam	4/5/15	21.54, -157.88	476 ± 23.8	349 ± 17.4
4	Oʻahu	Mauʻumae	4/3/15	21.29, -157,79	880 ± 44.0	785 ± 39.2
5	Oʻahu	Maunawili	4/4/15	21.41, -157.76	707 ± 35.4	625 ± 31.2
6	Oʻahu	Lyon Arboretum	5/30/15	21.37, -157.80	280 ± 14.0	186 ± 9.29
7	Oʻahu	UHM	6/1/15	21.30, -157.82	298 ± 14.9	257 ± 12.9
8	Oʻahu	Waikīkī	5/31/15	21.27, -157.82	479 ± 23.9	479 ± 23.9
9	Hawaiʻi	Kiholo Bay	11/12/15	19.85, -155.92	242 ± 12.1	233 ± 11.7
10	Hawaiʻi	Kiholo Bay	11/12/15	19.85, -155.92	144 ± 7.21	128 ± 6.41
11	Hawaiʻi	Kona	11/12/15	19.66, -155.98	140 ± 6.99	136 ± 6.81
12	Hawaiʻi	Cinder Cone	11/12/15	19.78, -155.92	229 ± 11.5	229 ± 11.4
13	Hawaiʻi	Waiaha Springs	11/12/15	19.637, -155.95	305 ± 15.3	275 ± 13.7
14	Hawaiʻi	Flume Road	1/17/16	19.59, -155.15	210 ± 10.5	158 ± 7.92
15	Hawaiʻi	Stainbeck Hwy	1/17/16	19.65, -155.08	110 ± 5.48	59.4 ± 2.97
16	Hawaiʻi	Pāhoa	1/17/16	19.45, -154.94	476 ± 23.8	195 ± 9.73
17	Hawaiʻi	MacKenzie Park	1/17/16	19.44, -154.86	133 ± 6.65	81.9 ± 4.09
18	Hawaiʻi	Volcano	1/17/16	19.45, -155.19	148 ± 7.38	87.2 ± 4.36
19	Hawaiʻi	Volcano	1/17/16	19.45, -1552.20	137 ± 6.81	109 ± 5.45
20	Hawaiʻi	Volcano	1/17/16	19.44, -155.22	198 ± 9.92	146 ± 7.29
21	Hawaiʻi	Volcano	1/17/16	19.44, -155.22	273 ± 13.7	112 ± 5.60
22	Hawaiʻi	Saddle Road	1/17/16	19.68, -155.19	230 ± 12.0	208 ± 10.4
23	Hawaiʻi	Saddle Road	1/17/16	19.67 -155.35	619 ± 30.9	614 ± 30.4
24	Hawaiʻi	Waikoloa	1/18/16	19.93, -155.78	116 ± 5.80	112 ± 5.61

Table 3.1.1. (Continued) Locations of soil sample collection, the date of collection, and pre and post drying weight (g).

ID	Island	Sample Location	Date Collected	Lat Lon	Wet Wt (g)	Dry Wt (g)
25	Hawaiʻi	Chinchuck Road	1/18/16	19.87, -155.16	158 ± 7.92	128 ± 6.41
26	Hawaiʻi	Kaiwiki Road	1/18/16	19.76, -155.16	200 ± 10.0	107 ± 5.34

Basalt samples were collected on the island of Hawaiʻi in 2016 in order to compare with previously analyzed samples (Cox & Fankhauser, 1984). Basalt sampling locations, collection date, and final sieved weight are tabulated in Table 3.1.2.

Table 3.1.2. Locations of basalt sample collection, the date of collection, and pre and post drying weight (g).

ID	Island	Sample Location	Date Collected	Lat Lon	Weight (g)
B1	Hawaiʻi	Saddle Road	1/17/16	19.68, -155.19	136 ± 6.78
B2	Hawaiʻi	Saddle Road	1/17/16	19.7, -155.44	129 ± 6.44

Mushrooms were collected on Oʻahu, the island of Hawaiʻi, and Kauaʻi between 2012-2013. Mushroom sampling locations, species or genera of the mushroom collected, collection date, and wet and dry weights are listed in Table 3.1.3.

Table 3.1.3. Locations of mushroom sample collection, the date of collection, species or genera of mushroom collected, and pre and post drying weight (g).

ID	Island	Sample Location	Species	Date Collected	Lat Lon	Wet Wt (g)	Dry Wt (g)
5	Oʻahu	Mānoa Falls	Polyporales sp.	11/11/12	21.34, -157.80	248 ± 12	102 ± 5.1
11	Oʻahu	Kahana Dam	Microporus affinis	1/6/13	21.54, -157.88	135 ± 7	56.46 ± 2.82
4	Oʻahu	HIG Courtyard	Unidentified	11/30/12	21.30, -157.82	340 ± 17	56.57 ± 2.83
3	Oʻahu	HIG Courtyard	Unidentified	11/9/12	21.98, -157.82	--	66.99 ± 3.35
8	Oʻahu	Dole St	Chlorophyllum molybdites	12/26/12	21.30, -157.82	66 ± 3	39.22 ± 1.96
21	Oʻahu	Makiki Valley	Unidentified	5/25/13	21.32, -157.83	232 ± 12	121.43 ± 6.10
22	Oʻahu	Makiki Valley	Unidentified	5/25/13	21.32, -157.83	272 ± 14	119.68 ± 5.98
23	Oʻahu	Kahana Valley	Earliella scabrosa	5/27/13	21.54, -157.89	250 ± 13	85.16 ± 4.26
24	Oʻahu	Kahana Valley	Microporus affinis	5/27/13	21.54, -157.89	264 ± 13	110.04 ± 5.50
25	Oʻahu	Kahana Dam	Microporus affinis	5/27/13	21.54, -157.88	182 ± 9	74.81 ± 3.74
18	Hawaiʻi	Mauna Kea Access Rd	Sullius brevipes	2/27/13	19.72, -155.45	498 ± 25	30.80 ± 1.54
19	Hawaiʻi	Saddle Rd	Gomphidium oregonensis	3/13/13	19.69, -155.45	324 ± 16	38.81 ± 1.94
26	Hawaiʻi	Waiakea Exp St	Unidentified	5/31/13	19.65, -155.08	282 ± 14	121.56 ± 6.08
28	Hawaiʻi	Waiakea Exp St	Earliella scabrosa	5/31/13	19.65 -155.08	362 ± 18	109.13 ± 5.46
29	Hawaiʻi	Waiakea Exp St	Marasmiellus inoderma	5/31/13	19.65, -155.08	200 ± 10	29.75 ± 1.49
30	Hawaiʻi	Stainbeck Hwy	Unidentified	5/31/13	19.59, -155.15	206 ± 10	50.97 ± 2.55
31	Hawaiʻi	Stainbeck Hwy	Unidentified	5/31/13	19.59, -155.15	335 ± 17	113.21 ± 5.66
33	Hawaiʻi	Kaiwiki Rd	Microporus flabelliformis	5/31/13	19.76, -155.16	432 ± 22	140.62 ± 7.03
34	Hawaiʻi	ChinChuck Rd	Microporus flabelliformis	5/31/13	19.87, -155.16	244 ± 12	89.81 ± 4.49
35	Hawaiʻi	MacKenzie Park	Auricularia sp.	6/01/13	19.44, -154.86	--	137.49 ± 6.87
1	Kauaʻi	Princeville	Lepiota besseyi	6/12/12	22.22, -159.49	--	22.08 ± 1.10
2	Kauaʻi	Wainiha	Merulius tremollosus	11/15/12	22.20, -159.56	107 ± 5	74.01 ± 3.70
9	Kauaʻi	Kōkeʻe State Park	Suillus brevipes	1/1/13	22.12, -159.71	--	59.39 ± 2.97
10	Kauaʻi	Waipa	Macrocybe spectabilis	12/28/12	22.20, -159.51	480 ± 24	51.68 ± 2.58

After sample collection, sample preparation, and gamma spectroscopy, ^{134}Cs and ^{137}Cs activities were decay corrected to March 2011 and compared to rainfall in March 2011 as shown in Table 3.1.4 and Table 3.1.5. All reported activities represent dry mass. Detectable ^{134}Cs activities ranged from 0.04 - 18 Bq/kg in soils and 0.24-7.2 Bq/kg in mushrooms. Detectable ^{137}Cs activities ranged from 0.32 – 52 Bq/kg in soils and 0.39 – 89 Bq/kg in mushrooms. ^{134}Cs was below the critical limit in the two basalt samples and ^{137}Cs ranged from 0.14 – 0.17 Bq/kg.

Table 3.1.4. ^{134}Cs and ^{137}Cs activities (Bq/kg) and CL's for soil samples collected on the islands of Oʻahu and Hawaiʻi decay corrected to March 20, 2011 and rainfall in mm for March 2011. Uncertainties reported are propagated to 2σ, or a 95% confidence interval.

ID	Island	Sample Location	^{134}Cs (Bq/kg)	^{134}Cs CL (Bq/kg)	^{137}Cs (Bq/kg)	^{137}Cs CL (Bq/kg)	Rainfall Mar. 2011 (mm)
6	Oʻahu	Lyon Arboretum	1.21 ± 0.35	0.01	42.86 ± 0.28	0.01	330.2 ± 40.4
2	Oʻahu	Mānoa Falls	1.62 ± 0.33	0.01	17.47 ± 0.17	0.01	309.6 ± 41.4
1	Oʻahu	Kahana Valley	<CL	0.01	4.86 ± 0.16	0.01	335.0 ± 57.7
4	Oʻahu	Mauʻumae	<CL	0.01	3.72 ± 0.08	0.01	136.5 ± 35.0
7	Oʻahu	HIG Courtyard	<CL	0.01	1.28 ± 0.05	0.01	124.8 ± 26.8
5	Oʻahu	Maunawili	<CL	0.01	0.39 ± 0.05	0.01	121.2 ± 21.0
3	Oʻahu	Kahana Dam	<CL	0.01	0.32 ± 0.05	0.01	289.7 ± 56.6
8	Oʻahu	Waikīkī	<CL	0.01	0.39 ± 0.04	0.01	68.5 ± 0.0
9	Hawaiʻi	Kiholo Bay	<CL	0.01	6.88 ± 0.11	0.01	31.9 ± 4.8
10	Hawaiʻi	Kiholo Bay	<CL	0.01	6.04 ± 0.10	0.01	31.9 ± 4.8
11	Hawaiʻi	Kona	<CL	0.01	1.32 ± 0.09	0.01	103.9 ± 18.8
12	Hawaiʻi	Cinder Cone	<CL	0.01	7.49 ± 0.10	0.01	67.0 ± 15.3
13	Hawaiʻi	Waiaha Springs	<CL	0.01	0.65 ± 0.07	0.01	99.8 ± 21.5
14	Hawaiʻi	Flume Road	2.15 ± 0.51	0.01	8.06 ± 0.21	0.01	571.7 ± 55.7
15	Hawaiʻi	Stainbeck Hwy	3.34 ± 0.63	0.02	22.45 ± 0.26	0.01	419.1 ± 36.0
16	Hawaiʻi	Pāhoa	0.80 ± 0.65	0.02	10.62 ± 0.25	0.01	345.0 ± 33.8
17	Hawaiʻi	MacKenzie Park	<CL	0.03	0.34 ± 0.04	0.02	259.7 ± 12.9
18	Hawaiʻi	Volcano	4.57 ± 1.55	0.02	49.53 ± 0.64	0.02	596.9 ± 54.3
19	Hawaiʻi	Volcano	17.64 ± 2.26	0.03	43.05 ± 0.70	0.02	555.6 ± 54.2
20	Hawaiʻi	Volcano	14.79 ± 2.80	0.03	51.64 ± 0.88	0.02	430.7 ± 53.2

Table 3.1.4. (Continued) ^{134}Cs and ^{137}Cs activities (Bq/kg) and CL's for soil samples collected on the islands of Oʻahu and Hawaiʻi decay corrected to March 20, 2011 and rainfall in mm for March 2011. Uncertainties reported are propagated to 2σ, or a 95% confidence interval.

ID	Island	Sample Location	^{134}Cs (Bq/kg)	^{134}Cs CL (Bq/kg)	^{137}Cs (Bq/kg)	^{137}Cs CL (Bq/kg)	Rainfall Mar. 2011 (mm)
21	Hawaiʻi	Volcano	4.97 ± 1.55	0.02	41.96 ± 0.61	0.02	420.2 ± 53.2
22	Hawaiʻi	Saddle Road	3.67 ± 0.45	0.01	41.90 ± 0.29	0.08	588.0 ± 50.6
23	Hawaiʻi	Saddle Road	<CL	0.01	2.55 ± 0.07	0.01	304.1 ± 52.6
24	Hawaiʻi	Waikoloa	<CL	0.01	2.90 ± 0.15	0.01	35.7 ± 21.4
25	Hawaiʻi	Chinchuck Rd	2.03 ± 0.47	0.01	3.63 ± 0.12	0.01	673.2 ± 38.2
26	Hawaiʻi	Kaiwiki Road	0.76 ± 0.42	0.01	6.52 ± 0.16	0.01	655.1 ± 42.1
B1	Hawaiʻi	Saddle Road	<CL	0.01	0.17 ± 0.05	0.005	591.7 ± 51.0
B2	Hawaiʻi	Saddle Road	<CL	0.01	0.14 ± 0.04	0.01	200.6 ± 32.9

Table 3.1.5. ^{134}Cs and ^{137}Cs activities and CL's (Bq/kg) for mushroom samples on the islands of Oʻahu, Hawaiʻi, and Kauaʻi decay corrected to March 20, 2011, rainfall in mm for March 2011. Uncertainties reported are propagated to 2σ, or a 95% confidence interval.

ID	Island	Sample Location	^{134}Cs (Bq/kg)	^{134}Cs CL (Bq/kg)	^{137}Cs (Bq/kg)	^{137}Cs CL (Bq/kg)	Rainfall Mar. 2011 (mm)
23	Oʻahu	Kahana Valley	<CL	0.04	4.79 ± 0.39	0.29	335.0 ± 57.7
24	Oʻahu	Kahana Valley	0.60 ± 0.07	0.04	3.34 ± 0.26	0.13	335.0 ± 57.7
5	Oʻahu	Mānoa Falls	1.56 ± 0.15	0.05	2.80 ± 0.23	0.19	303.8 ± 42.0
21	Oʻahu	Makiki Valley	1.33 ± 0.12	0.05	1.93 ± 0.16	0.07	178.2 ± 31.9
22	Oʻahu	Makiki Valley	0.83 ± 0.08	0.04	1.67 ± 0.14	0.11	178.2 ± 31.9
25	Oʻahu	Kahana Dam	0.70 ± 0.09	0.05	1.43 ± 0.12	0.18	335.0 ± 57.7
11	Oʻahu	Kahana Dam	0.72 ± 0.10	0.06	1.25 ± 0.12	0.30	289.7 ± 56.6
8	Oʻahu	Dole St	<CL	0.08	0.39 ± 0.08	0.18	107.5 ± 19.7
4	Oʻahu	HIG Courtyard	<CL	0.06	<CL	0.08	118.9 ± 25.2
3	Oʻahu	HIG Courtyard	<CL	0.08	<CL	0.05	118.9 ± 25.2
18	Hawaiʻi	Mauna Kea Access Rd	1.12 ± 0.19	0.03	88.99 ± 6.87	0.09	161.8 ± 29.6
19	Hawaiʻi	Saddle Rd	1.12 ± 0.19	0.03	30.05 ± 2.34	0.05	189.5 ± 32.3
26	Hawaiʻi	Waiakea Exp St	0.96 ± 0.11	0.03	19.52 ± 1.51	0.20	418.0 ± 35.3
28	Hawaiʻi	Waiakea Exp St	<CL	0.03	23.87 ± 1.84	0.25	418.4 ± 35.7
29	Hawaiʻi	Waiakea Exp St	7.51 ± 0.69	0.04	18.78 ± 1.49	0.11	419.1 ± 36.0
30	Hawaiʻi	Stainbeck Hwy	1.17 ± 0.14	0.03	4.20 ± 0.34	0.12	571.1 ± 55.7
31	Hawaiʻi	Stainbeck Hwy	0.48 ± 0.06	0.03	5.96 ± 0.47	0.26	571.1 ± 55.7
33	Hawaiʻi	Kaiwiki Rd	6.80 ± 0.67	0.04	20.27 ± 1.61	0.67	655.1 ± 42.1
34	Hawaiʻi	ChinChuck Rd	5.96 ± 0.54	0.04	9.43 ± 0.78	0.61	673.2 ± 38.2

Table 3.1.5. (Continued) ^{134}Cs and ^{137}Cs activities and CL's (Bq/kg) for mushroom samples on the islands of Oʻahu, Hawaiʻi, and Kauaʻi decay corrected to March 20, 2011, rainfall in mm for March 2011. Uncertainties reported are propagated to 2σ, or a 95% confidence interval.

ID	Island	Sample Location	^{134}Cs (Bq/kg)	^{134}Cs CL (Bq/kg)	^{137}Cs (Bq/kg)	^{137}Cs CL (Bq/kg)	Rainfall Mar. 2011 (mm)
35	Hawaiʻi	MacKenzie Park	0.24 ± 0.04	0.03	4.83 ± 0.38	0.17	259.7 ± 12.9
1	Kauaʻi	Princeville	1.48 ± 0.21	0.07	2.87 ± 0.26	0.17	195.2 ± 25.9
2	Kauaʻi	Wainiha	1.13 ± 0.11	0.06	1.64 ± 0.15	0.18	319.6 ± 52.2
9	Kauaʻi	Kōkeʻe State Park	1.97 ± 0.20	0.04	17.04 ± 1.33	0.06	125.4 ± 31.4
10	Kauaʻi	Waipa	<CL	0.05	8.14 ± 0.65	0.05	236.1 ± 30.9

In addition to radiocesium activity, ^{7}Be activity in soils and mushrooms were analyzed in order to confirm the validity of our proposed relationship between precipitation and radiocesium activity as shown in Table 3.1.6 and Table 3.1.7. Furthermore, secondary ROI were analyzed in soils to confirm that geochemical processes did not disrupt samples.

Table 3.1.6. Activities (Bq/kg) for secondary ROI in soils on the islands of Oʻahu and Hawaiʻi. ^{210}Pb is excess. ^{7}Be has been decay corrected to sample collection date. ^{40}K, ^{210}Pb, ^{238}U, and ^{226}Ra have not been decay corrected due to their long half-lives.

ID	Sample Location	^{40}K (Bq/kg)	^{7}Be (Bq/kg)	^{210}Pb (Bq/kg)	^{238}U (Bq/kg)	^{226}Ra (Bq/kg)
1	Kahana Valley	13.5 ± 1.4	8.5 ± 1.3	15.7 ± 0.4	6.2 ± 3.1	7.7 ± 0.6
2	Mānoa Falls	39.0 ± 1.8	20.5 ± 1.6	35.5 ± 0.2	20.9 ± 3.0	26.4 ± 0.8
3	Kahana Dam	26.7 ± 1.9	14.7 ± 1.6	0.0 ± 1.2	19.1 ± 4.0	15.6 ± 0.7
4	Mauʻumae	124.4 ± 2.3	5.9 ± 0.8	21.9 ± 0.3	11.8 ± 2.4	8.4 ± 0.5
5	Maunawili	110.9 ± 1.8	4.3 ± 0.9	0.0 ± 3.0	14.2 ± 2.7	15.1 ± 0.7
6	Lyon Arboretum	56.7 ± 1.9	20.7 ± 0.9	4.7 ± 0.2	41.8 ± 4.4	40.5 ± 0.9
7	HIG Courtyard	219.3 ± 2.0	12.2 ± 0.6	0.0 ± 3.8	15.8 ± 2.3	20.9 ± 0.5
8	Waikīkī	72.1 ± 1.5	4.2 ± 0.4	0.0 ± 2.7	13.7 ± 1.9	10.0 ± 0.4
9	Kiholo Bay	137.5 ± 2.9	4.8 ± 0.1	0.0 ± 0.8	4.7 ± 2.8	5.3 ± 0.5
10	Kiholo Bay	132.4 ± 1.9	11.3 ± 0.6	4.8 ± 0.8	4.0 ± 1.9	5.6 ± 0.4
11	Kona	143.6 ± 3.1	5.0 ± 0.9	10.9 ± 0.8	3.6 ± 2.9	4.1 ± 0.5
12	Cinder Cone	343.2 ± 3.0	2.4 ± 0.5	0.0 ± 0.8	8.1 ± 2.2	10.4 ± 0.4
13	Waiaha Springs	183.6 ± 3.5	36.7 ± 3.8	19.3 ± 0.4	2.7 ± 2.4	7.8 ± 0.7
14	Flume Road	79.7 ± 2.3	27.3 ± 1.5	169.4 ± 0.3	5.5 ± 3.4	2.2 ± 0.6
15	Stainbeck Hwy	73.0 ± 2.6	40.3 ± 2.5	191.8 ± 0.3	2.5 ± 3.8	8.7 ± 0.8
16	Pāhoa	129.2 ± 3.9	52.5 ± 2.5	7.2 ± 0.2	149.1 ± 4.2	5.1 ± 0.9
17	MacKenzie Park	64.8 ± 3.7	92.2 ± 1.8	200.1 ± 1.1	15.7 ± 6.8	1.0 ± 1.0
18	Volcano	118.8 ± 4.8	53.1 ± 4.1	421.2 ± 0.3	5.4 ± 5.9	3.7 ± 0.5
19	Volcano	85.2 ± 5.1	104.4 ± 6.1	847.1 ± 0.4	1.3 ± 6.0	2.5 ± 0.4
20	Volcano	107.5 ± 5.4	213.4 ± 7.0	498.5 ± 0.4	3.2 ± 7.2	3.2 ± 0.4
21	Volcano	78.7 ± 4.6	41.3 ± 4.4	265.0 ± 0.4	13.2 ± 6.1	2.8 ± 0.4

Table 3.1.6. (Continued) Activities (Bq/kg) for secondary ROI in soils on Oʻahu and the island of Hawaiʻi. ^{210}Pb is excess. ^{7}Be has been decay corrected to sample collection date. ^{40}K, ^{210}Pb, ^{238}U, and ^{226}Ra have not been decay corrected due to their long half-lives.

ID	Sample Location	^{40}K (Bq/kg)	^{7}Be (Bq/kg)	^{210}Pb (Bq/kg)	^{238}U (Bq/kg)	^{226}Ra (Bq/kg)
22	Saddle Road	92.74 ± 2.1	105.3 ± 2.4	200.1 ± 0.2	7.5 ± 3.3	3.3 ± 0.2
23	Saddle Road	0.00 ± 0.0	15.9 ± 1.0	13.6 ± 0.5	3.4 ± 1.9	2.7 ± 0.5
24	Waikoloa	346.56 ± 5.1	1.7 ± 0.2	4.6 ± 0.5	12.4 ± 3.2	14.4 ± 0.7
25	Chinchuck Rd	135.9 ± 2.8	88.8 ± 2.0	63.4 ± 0.2	7.0 ± 3.0	4.7 ± 0.6
26	Kaiwiki Road	73.9 ± 2.5	1.9 ± 0.2	24.0 ± 0.4	11.4 ± 3.2	7.8 ± 0.7

Table 3.1.7. Activity (Bq/kg) for ^{40}K in mushrooms on the islands of Oʻahu, Hawaiʻi, and Kauaʻi. ^{40}K was not decay corrected due to its long half-life.

ID	Island	Sample Location	^{40}K (Bq/kg)
5	Oʻahu	Mānoa Falls	50.0 ± 3.05
11	Oʻahu	Kahana Dam	72.7 ± 4.47
4	Oʻahu	HIG Courtyard	1160 ± 65.1
3	Oʻahu	HIG Courtyard	1180 ± 68.2
8	Oʻahu	Dole St	1160 ± 64.8
21	Oʻahu	Makiki Valley	172 ± 9.72
22	Oʻahu	Makiki Valley	135 ± 7.57
23	Oʻahu	Kahana Valley	100 ± 5.97
24	Oʻahu	Kahana Valley	86.8 ± 4.99
25	Oʻahu	Kahana Dam	84.5 ± 5.09
18	Hawaiʻi	Mauna Kea Access Rd	844 ± 47.6
19	Hawaiʻi	Saddle Rd	1180 ± 65.7
26	Hawaiʻi	Waiakea Exp St	38.5 ± 2.41
28	Hawaiʻi	Waiakea Exp St	39.9 ± 2.53
29	Hawaiʻi	Waiakea Exp St	1600 ± 90.2
30	Hawaiʻi	Stainbeck Hwy	1.28 ± 1.38
31	Hawaiʻi	Stainbeck Hwy	3.48 ± 0.760
33	Hawaiʻi	Kaiwiki Rd	57.4 ± 4.31
34	Hawaiʻi	ChinChuck Rd	75.0 ± 5.05
35	Hawaiʻi	MacKenzie Park	85.2 ± 4.91
1	Kauaʻi	Princeville	1180 ± 65.8
2	Kauaʻi	Wainiha	170 ± 9.77
9	Kauaʻi	Kōkeʻe State Park	641 ± 36.0
10	Kauaʻi	Waipa	1780 ± 108

Bulk Density and porosity measurements were conducted on soils and the results are shown in Table 3.1.8. Bulk densities ranged from 0.36 g/mL to 1.3 g/mL and percent porosities ranged from 20% to 76%.

The definitions for some soil characteristics were defined by the Hawaiʻi Soil Atlas (2014) and include potassium content, acidity, water holding capacity where potassium classification is based off both the concentration of potassium in the soil as well as its bulk density and texture and water holding capacity refers to the saturation point of the soil and is based off of permeability and water retention percentages. Water holding capacity classifications (in percentages) are defined as follows by the Hawaiʻi Soil Atlas (2014): low = 0-0.06, moderate = 0.07-0.13, high = 0.014-0.20, very high > 0.20. Table 3.1.9 summarizes, based off of these definitions, the soil characteristics for our soil samples.

Table 3.1.8. Soil bulk density and percent porosity measurements. * denotes value was not actually measured but instead inferred based off soil wet and dry weights.

ID	Island	Sample Location	Bulk Density (g/mL)	Porosity (%)
1	Oʻahu	Kahana Valley	0.91 ± 0.03	54.92
2	Oʻahu	Mānoa Falls	0.87 ± 0.02	42.21
3	Oʻahu	Kahana Dam	1.04 ± 0.02	45.21
4	Oʻahu	Mauʻumae	0.91 ± 0.02	44.26 54.76
5	Oʻahu	Maunawili	0.96 ± 0.02	54.76
6	Oʻahu	Lyon Arboretum	1.01 ± 0.03	51.90
7	Oʻahu	UHM	1.11 ± 0.03	55.30
8	Oʻahu	Waikīkī	1.11 ± 0.03	47.22
9	Hawaiʻi	Kiholo Bay	0.93 ± 0.22	33.44
10	Hawaiʻi	Kiholo Bay	1.15 ± 0.15	56.70
11	Hawaiʻi	Kona	1.13 ± 0.04*	47.21*
12	Hawaiʻi	Cinder Cone	1.13 ± 0.04	47.21
13	Hawaiʻi	Waiaha Springs	1.25 ± 0.11	46.43
14	Hawaiʻi	Flume Road	0.85 ± 0.03	57.13
15	Hawaiʻi	Stainbeck Hwy	1.00 ± 0.06	22.87
16	Hawaiʻi	Pāhoa	0.63 ± 0.02	51.77
17	Hawaiʻi	MacKenzie Park	0.36 ± 0.01	76.03
18	Hawaiʻi	Volcano	0.65 ± 0.04	71.38
19	Hawaiʻi	Volcano	0.71 ± 0.06	32.54
20	Hawaiʻi	Volcano	0.41 ± 0.10	64.23
21	Hawaiʻi	Volcano	0.52 ± 0.10	60.53
22	Hawaiʻi	Saddle Road	0.94 ± 0.02	34.68
23	Hawaiʻi	Saddle Road	1.31 ± 0.03	20.39
24	Hawaiʻi	Waikoloa	0.93 ± 0.14	61.14
25	Hawaiʻi	Chinchuck Rd	0.87 ± 0.05	28.60
26	Hawaiʻi	Kaiwiki Road	0.65 ± 0.03	45.35

Table 3.1.9. Soil characteristics identified from the Hawaiʻi Soil Atlas (2014).

ID	Island	Sample Location	Potassium Content	Water Holding Capacity	pH
1	Oʻahu	Kahana Valley	Sufficient	Moderate	4.4-5.0
2	Oʻahu	Mānoa Falls	Deficient	High	4.5-6.5
3	Oʻahu	Kahana Dam	Sufficient	Moderate	4.4-5.0
4	Oʻahu	Mauʻumae	No Data	High	6.6-7.3
5	Oʻahu	Maunawili	No Data	Moderate	5.1-6.5
6	Oʻahu	Lyon Arboretum	Deficient	High	4.5-6.5
7	Oʻahu	UHM	Deficient	High	5.1-5.5
8	Oʻahu	Waikīkī	No Data	Low	6.6-8.4
9	Hawaiʻi	Kiholo Bay	Abundant	High	6.1-7.3
10	Hawaiʻi	Kiholo Bay	Abundant	High	6.1-7.3
11	Hawaiʻi	Kona	Sufficient	High	6.1-7.3
12	Hawaiʻi	Cinder Cone	Sufficient	High	6.1-7.3
13	Hawaiʻi	Waiaha Springs	Sufficient	High	6.1-7.3
14	Hawaiʻi	Flume Road	Deficient	Very High	4.6-5.5
15	Hawaiʻi	Stainbeck Hwy	Deficient	Very High	4.6-5.5
16	Hawaiʻi	Pāhoa	Deficient	Moderate	5.1-5.5
17	Hawaiʻi	MacKenzie Park	Deficient	High	5.1-5.5
18	Hawaiʻi	Volcano	Deficient	Very High	3.5-4.4
19	Hawaiʻi	Volcano	Deficient	Very High	3.5-4.4
20	Hawaiʻi	Volcano	Deficient	Very High	3.5-4.4
21	Hawaiʻi	Volcano	Deficient	Very High	3.5-4.4
22	Hawaiʻi	Saddle Road	Deficient	Very High	4.6-5.5
23	Hawaiʻi	Saddle Road	Deficient	Moderate	4.5-5.5
24	Hawaiʻi	Waikoloa	Abundant	Low	6.1-7.3
25	Hawaiʻi	Chinchuck Rd	Deficient	Very High	4.5-6.0
26	Hawaiʻi	Kaiwiki Road	Deficient	Very High	4.5-6.0

Using the bulk density measurements and a sampling volume of 25 cm^3, cesium inventories were also converted to units of Bq/m^2 (Table 3.1.10). Detectable ^{134}Cs inventories ranged from 18 Bq/m^2 to 620 Bq/m^2 and ^{137}Cs inventories ranged from 18 Bq/m^2 to 2200 Bq/m^2.

Table 3.1.10. Cesium inventories per area (Bq/m^2).

ID	Island	Sample Location	^{134}Cs (Bq/m^2)	^{137}Cs (Bq/m^2)
1	Oʻahu	Kahana Valley	<CL	210.6 ± 8.9
2	Oʻahu	Mānoa Falls	74.2 ± 15.1	798.2 ± 21.5
3	Oʻahu	Kahana Dam	<CL	115.2 ± 2.6
4	Oʻahu	Mauʻumae	<CL	193.5 ± 6.6
5	Oʻahu	Maunawili	<CL	17.7 ± 2.2
6	Oʻahu	Lyon Arboretum	60.9 ± 17.7	2154.7 ± 59.9
7	Oʻahu	UHM	<CL	71.3 ± 3.21
8	Oʻahu	Waikīkī	<CL	21.5 ± 2.52
9	Hawaiʻi	Kiholo Bay	<CL	320.5 ± 75.0
10	Hawaiʻi	Kiholo Bay	<CL	346.4 ± 46.5
11	Hawaiʻi	Kona	<CL	74.42 ± 5.5
12	Hawaiʻi	Cinder Cone	<CL	423.8 ± 14.5
13	Hawaiʻi	Waiaha Springs	<CL	40.5 ± 5.6
14	Hawaiʻi	Flume Road	91.0 ± 21.9	341.4 ± 13.7
15	Hawaiʻi	Stainbeck Hwy	252.0 ± 36.8	1125.4 ± 69.4
16	Hawaiʻi	Pāhoa	25.3 ± 20.5	336.8 ± 14.3
17	Hawaiʻi	MacKenzie Park	<CL	63.5 ± 3.7
18	Hawaiʻi	Volcano	149.4 ± 29.1	1620.4 ± 94.9
19	Hawaiʻi	Volcano	624.6 ± 67.7	1524.7 ± 129.4
20	Hawaiʻi	Volcano	302.2 ± 81.0	1055.3 ± 266.9
21	Hawaiʻi	Volcano	130.1 ± 34.7	1097.2 ± 220.0
22	Hawaiʻi	Saddle Road	172.7 ± 21.9	1970.9 ± 53.7
23	Hawaiʻi	Saddle Road	17.7 ± 18.1	166.6 ± 6.2
24	Hawaiʻi	Waikoloa	<CL	134.3 ± 21.8
25	Hawaiʻi	Chinchuck Road	87.6 ± 20.9	156.8 ± 10.1
26	Hawaiʻi	Kaiwiki Road	24.7 ± 13.5	210.6 ± 10.7

CHAPTER 4. DISCUSSION

4.1. Soil characteristics

Soil characteristics are known to heavily influence cesium absorption by biota as well as influence processes such as leeching (Fujii et al., 2014). In this study, we did not characterize soils but relied on information from the literature for each respective region where samples were obtained. Thus it is possible that local samples differ from regional soil maps. We found that all soils with detectable ^{134}Cs inventories were deficient in potassium as based off the Hawai'i Soil Atlas. Furthermore, all soils but one with detectable ^{134}Cs were acidic and had a high to very high water holding capacity. These variables are not independent as it is possible that soil characteristics are driven by rainfall. To show this Figures 4.1.1, 4.1.2, and 4.1.3. present the statistical variation of ^{134}Cs activity ,^{137}Cs activity, and March 2011 rainfall with respect to potassium content.

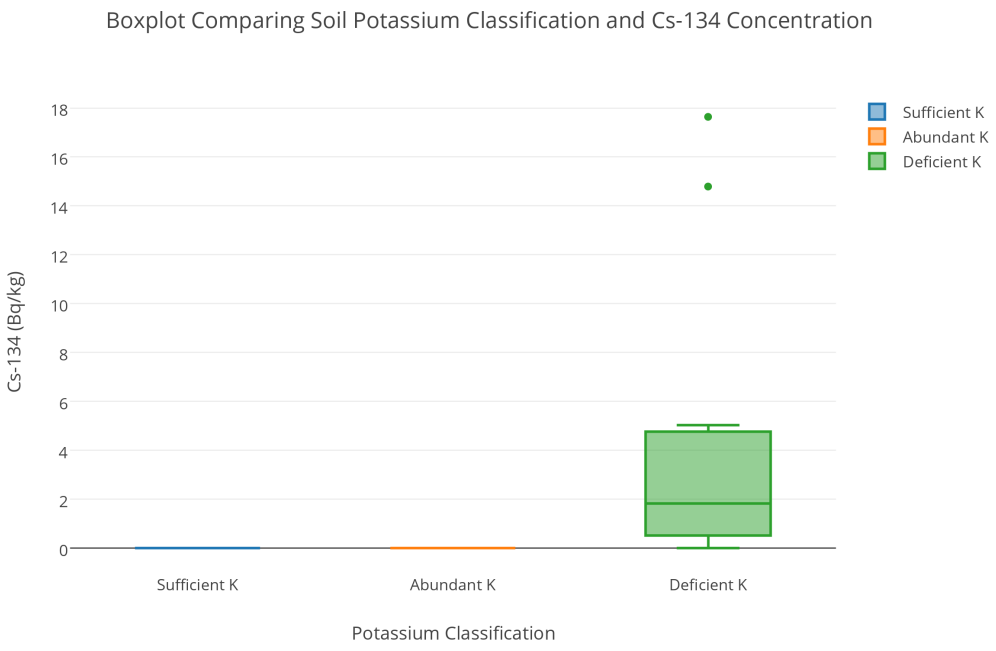

Figure 4.1.1. Box and whisker plot of ^{134}Cs (Bq/kg) with respect to potassium classification in soils.

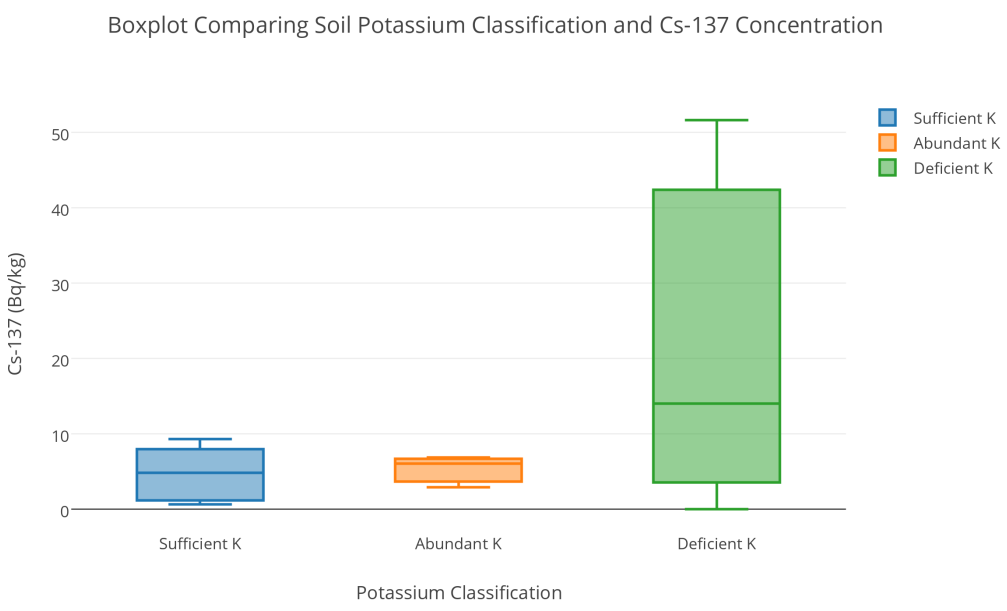

Figure 4.1.2. Box and whisker plot of ^{137}Cs (Bq/kg) with respect to potassium classification in soils.

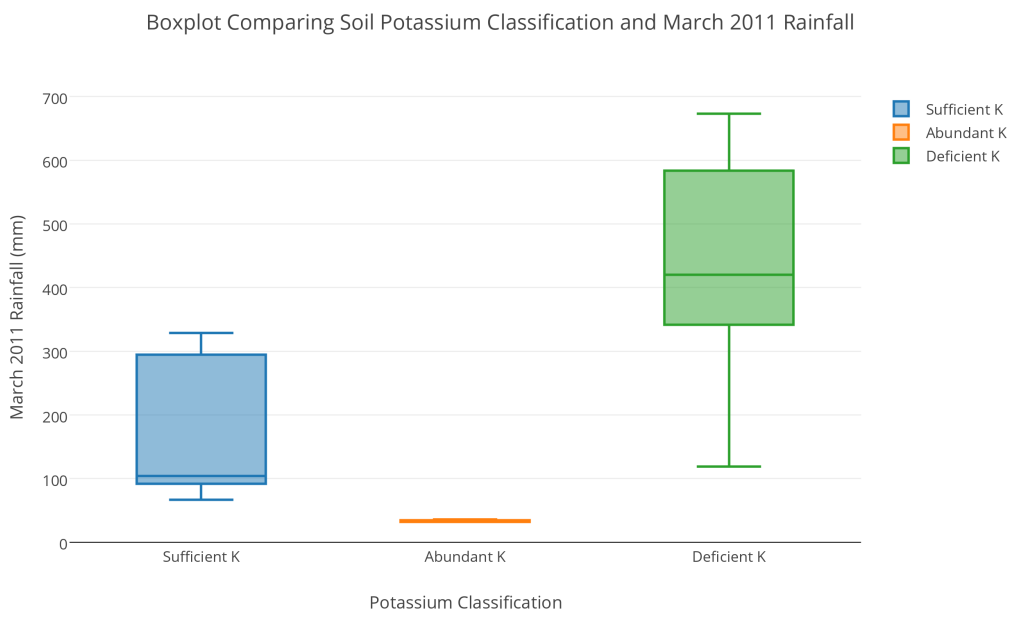

Figure 4.1.3. Box and whisker plot of March 2011 rainfall (mm) with respect to potassium classification in soils.

When present, radiocesium inventories were not correlated with potassium content inferred by ^{40}K, this may be due to cesium enrichment of soils with potassium deficiency and other factors such as canopy cover that would affect cesium deposition but not ^{40}K (Figure 4.1.4).

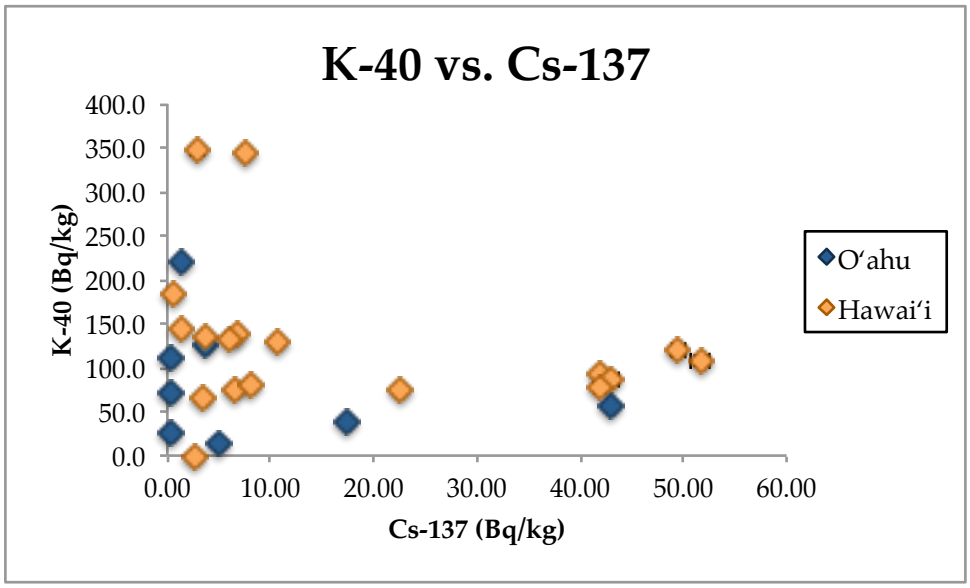

Figure 4.1.4. ^{40}K versus ^{137}Cs activity in Bq/kg in soils.

Higher potassium inventories have also previously shown to positively influence cesium uptake by mushrooms (Seeger, 1978). No correlation between ^{40}K and ^{137}Cs inventories, however, were found in this study (Figure 4.1.5). This may be due to variable canopy cover and uptake rate between the various mushroom species.

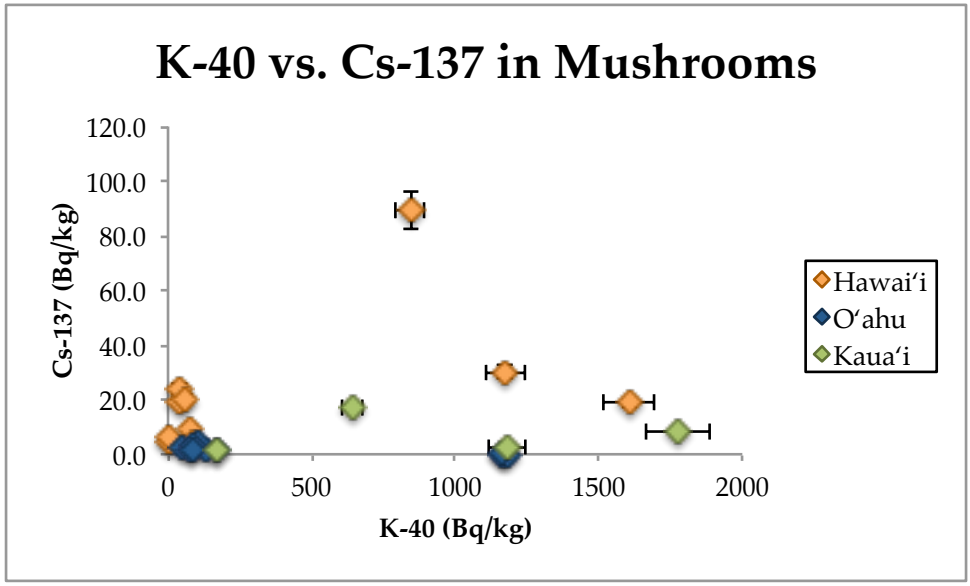

Figure 4.1.5. ^{40}K versus ^{137}Cs activity in Bq/kg in mushrooms.

4.2. Fukushima-derived fallout in soils

Higher rainfall in March 2011 resulted in elevated Fukushima-derived cesium in soils on the islands of O'ahu and Hawai'i along some of the studied transects as shown in Figures 4.2.1 and 4.2.2. Our detectable Fukushima-derived soil inventories ranged from 18 Bq/m^2 to 625 Bq/m^2. For comparison, up to 102,000 Bq/m^2 of ^{137}Cs was detected in forest soils analyzed near the FDNPP (Kato et al., 2012)

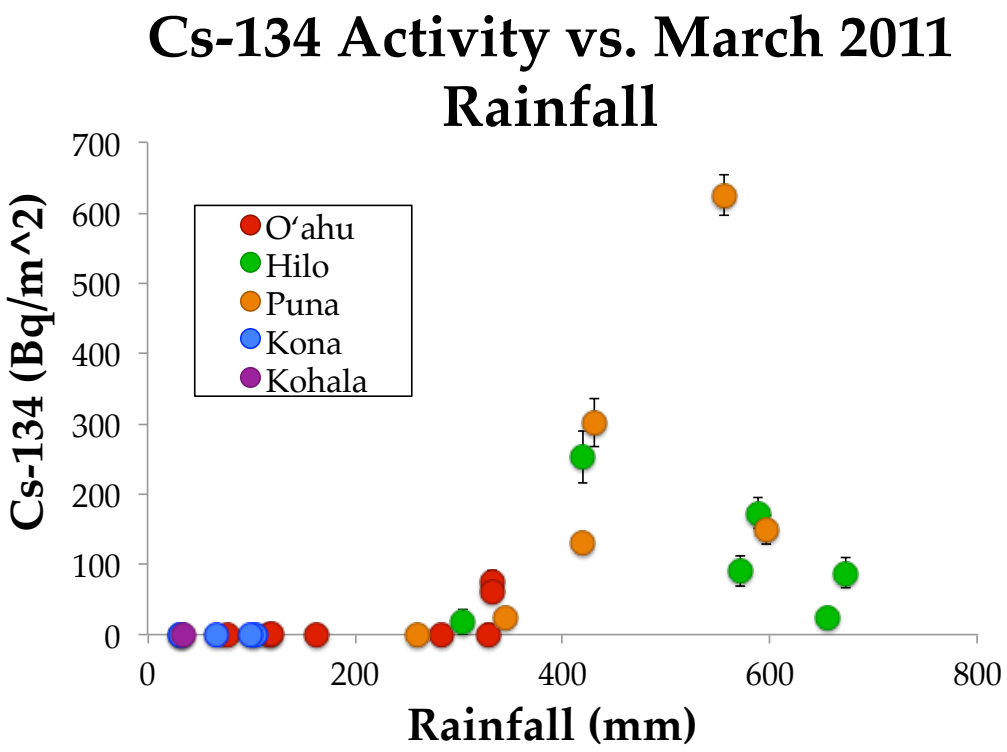

Figure 4.2.1. March 2011 rainfall in mm vs. ^{134}Cs activity for samples collected on the islands of O'ahu and Hawai'i. Activities have been decay corrected to March 2011, the month of the Fukushima disaster.

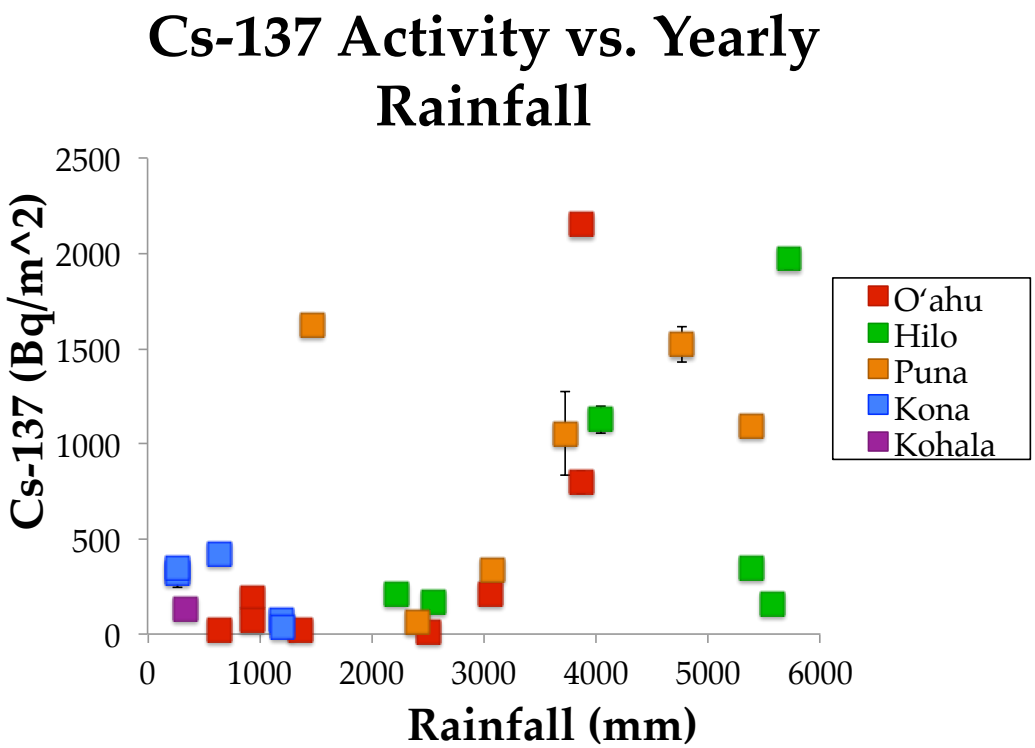

Figure 4.2.2. Annual 2011 rainfall in mm vs. ^{137}Cs activity for samples collected on the islands of O'ahu and Hawai'i. Activities have been decay corrected to March 2011, the month of the Fukushima disaster.

While all soil samples had ^{137}Cs there were some that had very little fallout contribution from new cesium sources. Soil samples with detectable Fukushima-derived cesium inventories were compared to the total cesium inventories (Figure 4.2.3). The Fukushima-derived cesium ranged from 5% to 72% for our samples. Most of the samples were comprised of under 30% Fukushima-derived cesium meaning historical fallout made up the majority of the overall soil radiocesium inventory.

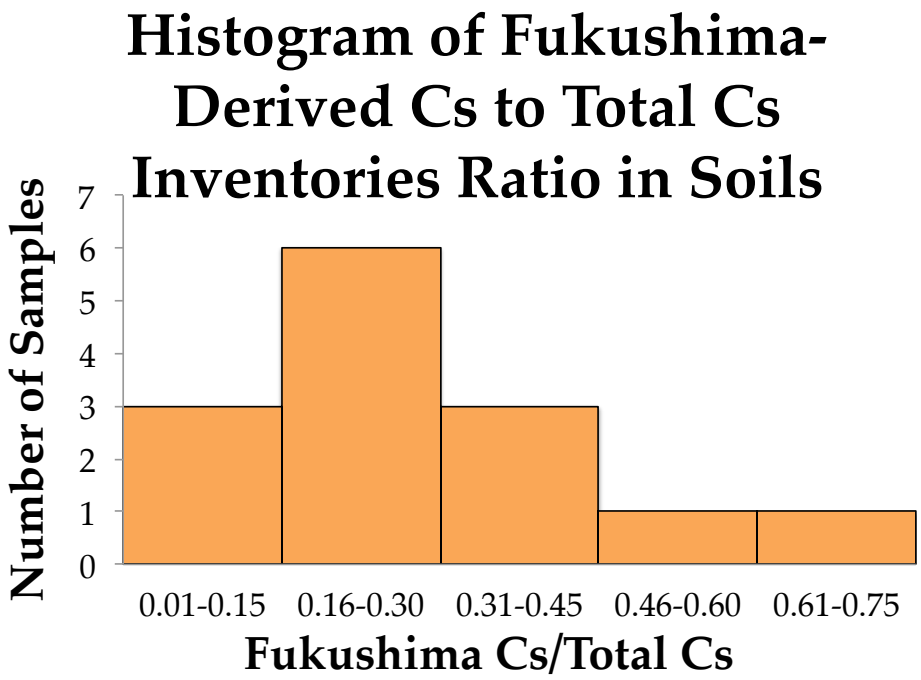

Figure 4.2.3. Histogram of Fukushima-derived cesium to total cesium ratio for soil samples collected on the islands of Oʻahu and Hawaiʻi.

Using the particulate ^{131}I to ^{137}Cs average ratio of 7.3 ± 2.8 in aerosols found by the EPA's RADNET system, ^{131}I deposition was also estimated and found to range from 130 to 4570 Bq/m^2.

<u>Oʻahu - Soils</u>

On Oʻahu, only two soil samples out of seven had detectable ^{134}Cs. These samples were all located in the Mānoa Valley and ranged from 61 to 74 Bq/m^2. Moreover, it appears that the leeward side of the island where Mānoa Valley is located was subject to a larger deposition of cesium in comparison to Kahana Valley that is located on the windward side and had much lower to

non-detectable levels of ^{134}Cs. While both areas were subject to similar rainfall amounts in March 2011, these differences can be explained by differences in canopy cover and soil characteristics. The soil samples located in Mānoa Valley were collected in low to moderate canopy cover and classified as deficient in potassium and as having a high water holding capacity (Hawaiʻi Soil Atlas, 2014). This is as opposed to the soil samples collected in Kahana Valley, which were under moderate to heavy canopy cover and classified as sufficient in potassium, acidic, and having a moderate water holding capacity (Hawaiʻi Soil Atlas, 2014). The deviation from our expected result of Kahana Valley having higher soil cesium inventories compared to Mānoa Valley can be explained by the differences in soil characteristics as well as canopy cover differences.

Other samples collected on Oʻahu did not have detectable ^{134}Cs and were subject to the lowest March 2011 rainfall for samples on Oʻahu. This included two samples from areas subject to lower rainfall in Honolulu and one sample collected from Maunawili. ^{137}Cs inventories in these samples ranged from 18 Bq/m^2 to 190 Bq/m^2.

Hawai‘i – Overview of Soils

On the island of Hawai‘i, four different areas included both the windward and the leeward sides of the island were studied. The areas studied on the windward side include Hilo and Puna and include samples from Saddle Road, Hilo, Puna, Volcano, and Pāhoa. On the leeward side, samples were taken from the Kona area and Waikoloa.

Hawai‘i – Hilo Soils

Soils collected from the Hilo area were subject to high rainfall. Figure 4.2.4 highlights cesium activies with relation to rainfall for soils collected in the Hilo area.

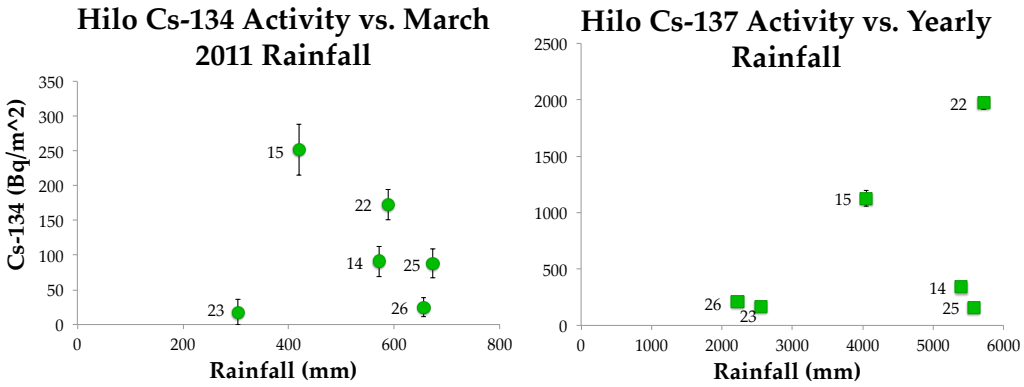

Figure 4.2.4. Hilo area soil ^{134}Cs inventories (Bq/m^2) vs. March 2011 rainfall and ^{137}Cs inventories (Bq/m^2) vs. Annual 2011 rainfall. Specific samples are referred to by number.

The soils collected in northern Hilo both had measurable Fukushima-derived fallout and include Chinchuck Road (sample 25) and Kaiwiki Road (sample 26). These samples were subject to similar rainfall and are part of the same soil series (Hawai'i Soil Atlas, 2014), however, their ^{134}Cs and ^{137}Cs activities were lower than expected based on the trends suggested by the other samples of similar rainfall, which can be attributed to differences in canopy cover. Soil collected from Kaiwiki was under dense canopy cover compared to the soil collected at Chinchuck, which was only partially obstructed. ^{134}Cs activities decay corrected to March 20, 2011 were 25 Bq/m^2 and 88 Bq/m^2 for Kaiwiki and Chinchuck respectively. ^{137}Cs activities, however, did not follow our expected trend of a positive relationship between rainfall and cesium deposition. ^{137}Cs activities were 210 Bq/m^2 and 160 Bq/m^2 for Kaiwiki and Chinchuck respectively, meaning Kaiwiki was subject to much higher levels of historical fallout compared to Chinchuck. This difference in fallout distribution may be attributed to several causes, including changes in canopy cover or historical local rainfall differences.

Soils collected from southern Hilo include samples from Flume Road (Sample 14) and Stainbeck Highway (Sample 15). The soils we collected from southern Hilo are deficient in potassium, acidic, and have a very high water holding capacity (Hawai'i Soil Atlas, 2014). Sample 14 from Flume Road, which was subject to higher March 2011 rainfall, had a ^{134}Cs activity of 91 Bq/m^2 and a ^{137}Cs activity of 340 Bq/m^2. This soil was partially obstructed by canopy cover at the time of collection. Sample 15 from Stainbeck Highway

was subject to lower March 2011 rainfall and had a ^{134}Cs activity of 250 Bq/m^2 and a ^{137}Cs activity of 1130 Bq/m^2. Unlike the soil collected at Flume Road, this sample was not obstructed by canopy cover, which likely explains the higher cesium inventory found.

Saddle Road soil samples were collected along two different precipitation gradients and have differing soil characteristics according to the Hawaiʻi Soil Atlas. Sample 22, which was subject to higher March 2011 rainfall and was partially obstructed by canopy cover, had a ^{134}Cs activity of 170 Bq/m^2 and a ^{137}Cs activity of 1970 Bq/m^2. This soil is classified as being deficient in potassium, acidic, and as having a very high water holding capacity (Hawaiʻi Soil Atlas, 2014). In comparision, sample 23 which was also not obstructed by canopy cover, had a ^{134}Cs activity of 18 Bq/m^2 and a ^{137}Cs activity of 170 Bq/m^2. This soil is classified as being deficient in potassium, neutral acidity, and having a moderate water holding capacity (Hawaiʻi Soil Atlas, 2014). The trends observed between these samples met our expectations of higher cesium depostion with higher rainfall. Furthermore, we also expected to find higher cesium inventories in soils which are acidic, which is also what we saw along this transect.

Hawai‘i – Puna Soils

Soil samples collected from Puna represent a variety of rainfall and soil characteristics. Radiocesium activities vs. rainfall for the Puna area are highlighted in Figure 4.2.5.

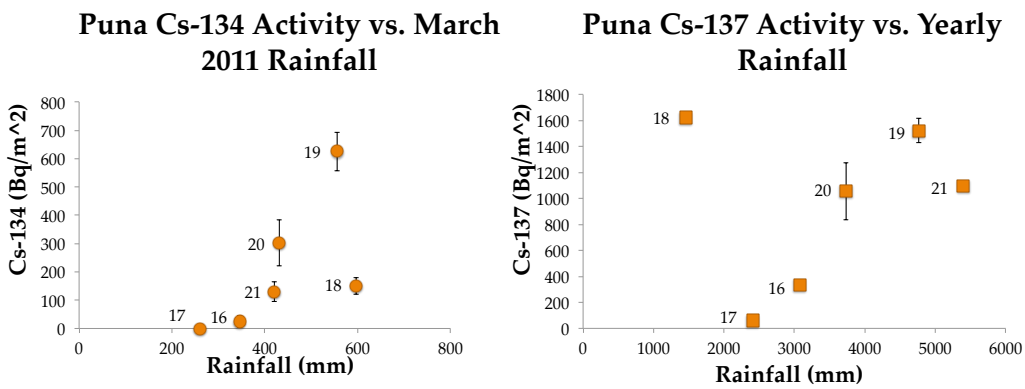

Figure 4.2.5. Soil ^{134}Cs inventories (Bq/m^2) vs. March 2011 rainfall and ^{137}Cs inventories (Bq/m^2) vs. Annual 2011 rainfall for the Hilo area. Specific samples are referred to by number.

Soil samples from Volcano were subject to high rainfall. Four samples were collected in Volcano, and represent different precipitation gradients and canopy cover conditions, but similar soil characteristics. Soils collected in this area are deficient in potassium, acidic, and have a very high water holding capacity (Hawai‘i Soil Atlas, 2014). Sample 18 was subject to the highest March 2011 rainfall and the lowest yearly rainfall in the Volcano area. This sample was partially obstructed by canopy cover. Radioactivities measured were 150 Bq/m^2 and 1600 Bq/m^2 for ^{134}Cs and ^{137}Cs, respectively.

The discrepancy between the expected relationship between rainfall and ^{134}Cs deposition may be attributed to obstruction by canopy cover. Sample 18 was also interesting because of its higher ^{137}Cs inventory in relation to annual rainfall. This highlights an alternative process which may have affected this location where surface runoff from higher elevations allows rainwater to pool in this location. Sample 19 was subject to the second highest rainfall in the Volcano area, was not obstructed by canopy cover, and had the highest ^{134}Cs activity for all soils measured in this study. This sample had 620 Bq/m^2 of ^{134}Cs and 1500 Bq/m^2 of ^{137}Cs. Samples 20 and 21 were both partially obstructed by canopy cover, but to a lesser degree than Sample 19. Sample 20 had a ^{134}Cs inventory of 300 Bq/m^2 and a ^{137}Cs inventory of 1100 Bq/m^2. Sample 21 had a ^{134}Cs inventory of 130 Bq/m^2 and a ^{137}Cs inventory of 1100 Bq/m^2. The trends seen in Volcano suggest that canopy cover is an important factor for atmospheric cesium depostion. Samples collected here did not follow our expected correlation between cesium deposition and precipitation and it is assumed the forest canopy caught the fallout.

Two soil samples were collected from the Pāhoa area, samples 16 and 17 and were subject to lower to moderate amounts of March 2011 rainfall (Hawaiʻi Rainfall Atlas, 2011). Both of these soils are classified as deficient in potassium and having neutral acidity (Hawaiʻi Soil Atlas, 2014). Sample 16, which was underneath full canopy cover, had 25 Bq/m^2 of ^{134}Cs and 340 Bq/m^2 of ^{137}Cs. This soil is classified as having a moderate water holding

capacity (Hawaiʻi Soil Atlas, 2014). Sample 17, which was underneath partial canopy cover and subject to lower March 2011 rainfall did not have detectable ^{134}Cs and had 64 Bq/m^2 of ^{137}Cs. This soil is classified as having a high water holding capacity (Hawaiʻi Soil Atlas, 2014).

Hawaiʻi – Leeward Soils

None of the samples collected from the leeward side of the island of Hawaiʻi had detectable ^{134}Cs. This is expected because the leeward side is subject to much lower rainfall amounts. ^{137}Cs inventories ranged from 41 Bq/m^2 to 420 Bq/m^2. Soils collected from this area are ranked as either sufficient or abundant in potassium, having neutral acidity, and as having a low to high water holding capacity (Hawaiʻi Soil Atlas, 2014).

4.3. Fukushima-derived fallout in mushrooms

Cesium in mushrooms was much more detectable because they bioaccumulate cesium and thus concentrate cesium. Cesium activities in mushrooms from the islands of Oʻahu, Hawaiʻi, and Kauaʻi are shown in Figure 4.3.1.

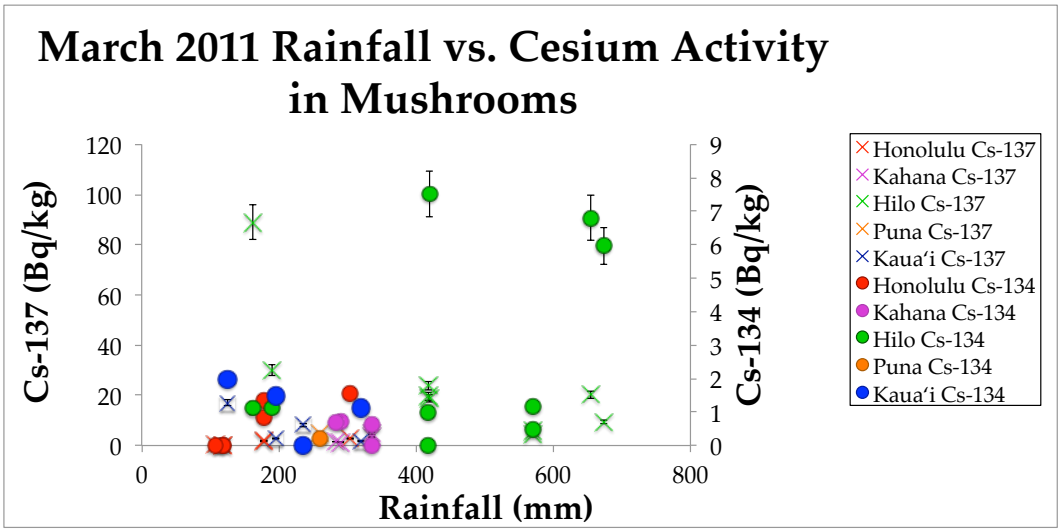

Figure 4.3.1. March 2011 rainfall in mm vs. Radiocesium activity in Bq/kg for samples collected on the islands of O'ahu and Hawai'i (both ^{137}Cs and ^{134}Cs). Activities have been decay corrected to March 2011, the month of the Fukushima disaster.

A strong relationship between soil and mushroom cesium inventories was not found when comparing locations where both soil and mushroom were collected (Figure 4.3.2). A general relationship, however, can be observed between soil and mushroom cesium inventories.

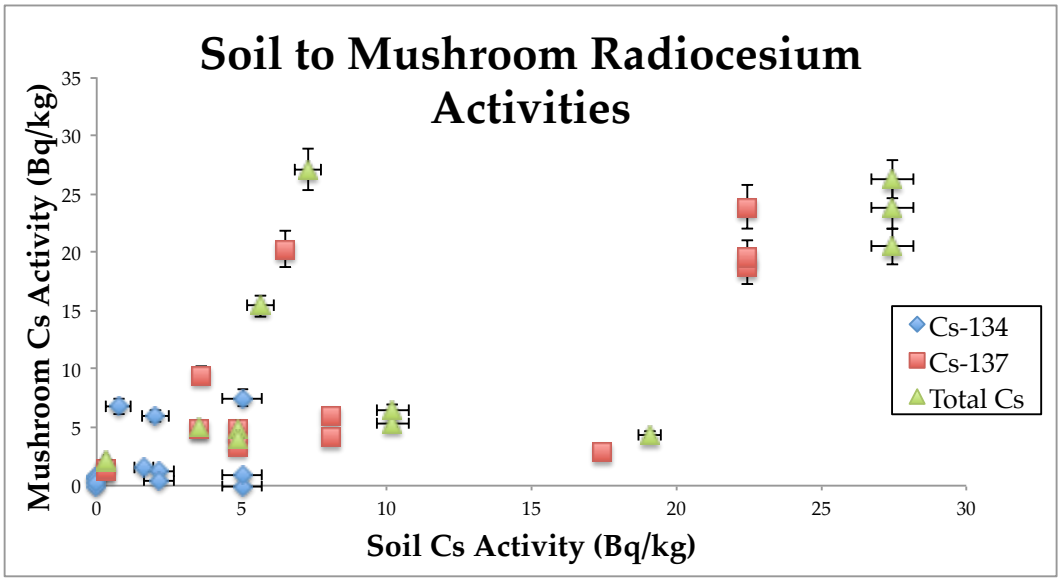

Figure 4.3.2. Comparison of soil to mushroom ^{134}Cs, ^{137}Cs, and total Cs in Bq/kg.

<u>O'ahu - Mushrooms</u>

On O'ahu, we found that the mushroom activities generally were correlated with higher precipitation rates. Mushrooms produced a more pronounced trend then the one seen in soils of O'ahu where higher precipitation rates in March 2011 resulted in increased cesium activities in mushrooms. Even in locations where we were not able to detect cesium in soils, mushrooms show a clear ^{134}Cs signature both on the leeward and windward sides of the island on O'ahu and the windward side of Hawai'i. We found that detectable ^{134}Cs inventories ranged from 0.60 Bq/kg to 1.6 Bq/kg and ^{137}Cs inventories ranged from 0.39 Bq/kg to 4.8 Bq/kg.

In the Kahana Valley, which is subject to higher rainfall, we found ^{134}Cs activities ranging from below CL to 0.70 Bq/kg. Two of the samples from the Kahana Valley were identified as Microporous affinis and these mushrooms exhibited similar cesium inventories for both ^{134}Cs and ^{137}Cs. ^{137}Cs was 1.3 Bq/kg to 1.4 Bq/kg and ^{134}Cs was 0.70 Bq/kg to 0.72 Bq/kg in these mushrooms. Two other samples were collected in the same location in Kahana Valley area, one that was identified as Earliella scabrosa and another that was not identified. The Earliella scabrosa sample was collected growing off of a tree and not soil and did not have detectable ^{134}Cs and had 4.8 Bq/kg of ^{137}Cs. The unidentified species had detectable a ^{134}Cs activity of 0.60 Bq/kg and a ^{137}Cs activity of 3.3 Bq/kg. The differences in new cesium inventories in these samples are likely the product of differing growing substrates. The differences in old cesium inventories are likely due to the differing bioaccumulation rates of different mushroom species.

On the leeward side of Oʻahu, we collected mushroom samples in the Makiki and Mānoa Valleys. In the Makiki Valley, we collected two unidentified mushroom species, which had similar activities of ^{134}Cs and ^{137}Cs. ^{134}Cs was 0.83 Bq/kg and 1.3 Bq/kg and ^{137}Cs was 1.7 Bq/kg and 1.9 Bq/kg. In Mānoa Valley, we found detectable ^{137}Cs activities that ranged from 0.39 Bq/kg to 2.8 Bq/kg and detectable ^{134}Cs activities were 1.6 Bq/kg. Two unidentified mushroom samples growing on trees were collected from the University of Hawaiʻi at Mānoa. Both of these samples did not have detectable cesium inventories. One unidentified mushroom sample was collected from

Mānoa Falls, an area subject to higher rainfall. As expected, that mushroom also had a higher radiocesium inventory of 1.6 Bq/kg and 2.8 Bq/kg of ^{134}Cs and ^{137}Cs, respectively.

We compared Fukushima-derived radiocesium activities to the total radiocesium inventory on O‘ahu and found a range of 31% to 81% Fukushima-derived cesium with most samples ranging from 61% to 75% as shown in Figure 4.3.3.

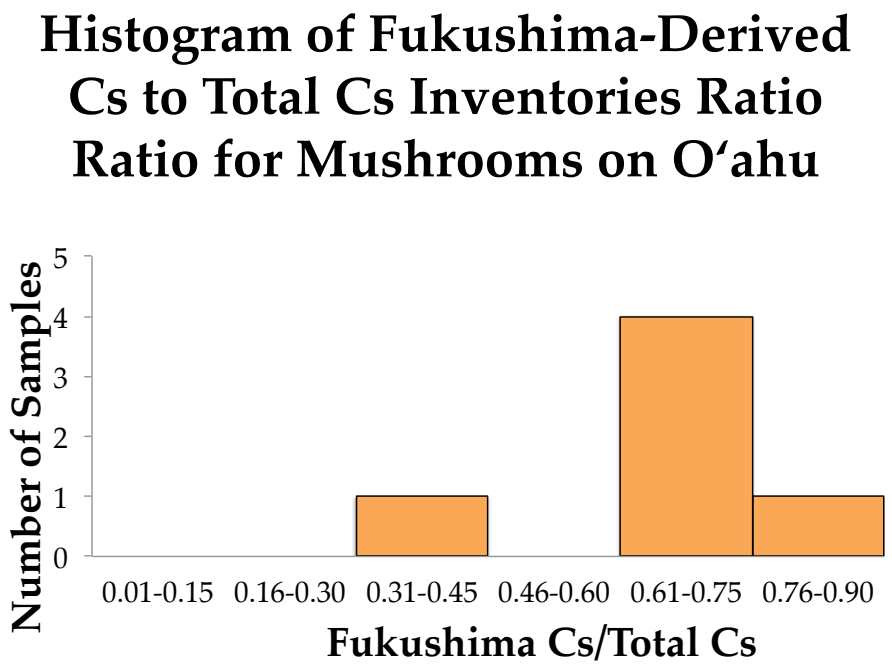

Figure 4.3.3. Histogram of Fukushima-derived to total cesium ratio for mushroom samples collected on O‘ahu. Most samples were comprised of 61-75% Fukushima-derived cesium.

This suggests that soil conditions or canopy cover may have changed in a lot of the areas where mushrooms were collected as we expected to see ^{134}Cs making up a much smaller portion of the overall radiocesium inventory from our soil measurements.

Hawaiʻi - Mushrooms

On the island of Hawaiʻi, samples were only collected on the windward side of the island and primarily in the Hilo area. Mushrooms collected on the island of Hawaiʻi generally followed the expected trend of increased cesium deposition with increased rainfall. Detectable ^{134}Cs and ^{137}Cs inventories ranged from 0.24 Bq/kg to 7.5 Bq/kg and 4.8 Bq/kg to 89 Bq/kg, respectively.

Mushrooms collected from the South Hilo area had a range of detectable ^{134}Cs deposition from 0.48 Bq/kg to 7.5 Bq/kg. ^{137}Cs inventories ranged 4.2 Bq/kg to 89 Bq/kg and overall higher ^{137}Cs activities did not correspond the higher ^{134}Cs activities, which is likely the product of differing soil and canopy cover conditions for historical fallout. Furthermore, the mushroom with the highest ^{134}Cs activity came from the South Hilo area and was of the Marasmiellus inoderma species.

Mushrooms collected from the North Hilo area at Chinchuck and Kaiwiki Roads had higher ^{134}Cs activities ranging from 6.0 Bq/kg to 6.8 Bq/kg and were subject to the highest rainfall in March 2011 of all

mushroom samples taken. Both mushrooms were of the same species, Microporous flabelliformis. Moreover, these mushrooms had differing ^{134}Cs to ^{137}Cs ratios, consistent with what was found in the soil samples. Mushroom samples Fukushima-derived cesium to total cesium ratios were 50% and 77% for Kaiwiki and Chinchuck respectively. Kaiwiki Road soil and mushroom samples had higher ^{137}Cs deposition historically compared to soil and mushroom samples collected at Chinchuck Road.

We also compared ^{134}Cs to ^{137}Cs activities on the island of Hawaiʻi and found a wider range compared to Oʻahu as shown in Figure 4.3.4. The ratio between Fukushima-derived cesium and total cesium ranged from 2% to 77%.

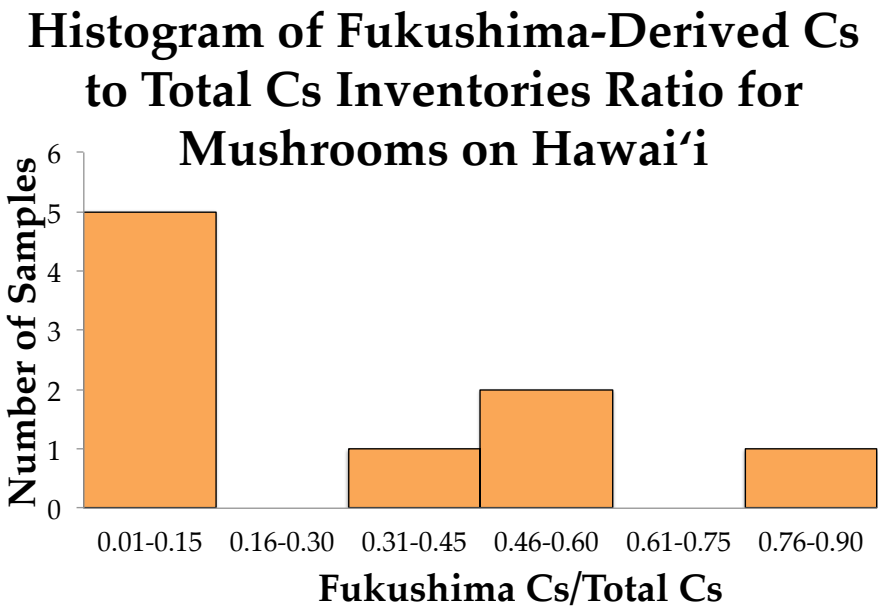

Figure 4.3.4. Histogram of Fukushima-derived to total cesium activities for mushrooms on the island of Hawaiʻi. Most samples comprised of 1% - 15% Fukushima-derived cesium.

Kaua‘i - Mushrooms

Mushrooms from differing precipitation gradients, canopy coverage, and species were also collected on the island of Kaua‘i and detectable ^{134}Cs inventories ranged from 1.1 Bq/kg to 2.0 Bq/kg and ^{137}Cs inventories ranged from 1.6 Bq/kg to 17 Bq/kg. Cesium inventories were not well correlated with March 2011 precipitation, which likely can be attributed to differences in soil characteristics.

While bioaccumulation happens at different rates within species, mushrooms still show a generally positive trend of precipitation driven cesium deposition that is also heavily influenced by canopy cover and substrate characteristics.

4.4 Pre vs. Post Fukushima Soil Contamination

Activities from Cox & Fankhauser (1984) reported for soil samples were decay corrected to March 2011 to estimate ^{137}Cs activities from nuclear weapons testing fallout that still remain today. Cox & Fankhauser’s measured activities were compared to cesium activities measured in this study in order to confirm that the levels detected in soils without ^{134}Cs today have ^{137}Cs activities predicted based on Cox and Fankhauser’s study. ^{137}Cs activities measured in this study largely are a product of nuclear weapons testing, and not the Fukushima disaster. In comparison, decay-corrected to March 20, 2011 ^{137}Cs activities from Cox and Fankhauser’s study ranged from 0.020

Bq/kg to 35 Bq/kg. This study found decay-corrected ^{137}Cs concentrations to range from 0.34 Bq/kg to 52 Bq/kg. Because ^{134}Cs and ^{137}Cs were released from Fukushima in a near 1:1 ratio, ^{134}Cs activities best reflect Fukushima-derived cesium wet deposition, which ranged from 0.27 Bq/kg to 18 Bq/kg. A comparison of Cox & Fankhauser's measurements to our measurements is shown in Figure 4.4.1. Decay correction of Cox & Fankhauser values and our values to 2011 confirmed our assumption of low cesium migration in sediments for most samples. Some samples had comparatively higher ^{137}Cs activities and there are several possibilities for this, including slight differences in sampling location or changes in canopy cover or land use in the last 50 years. Overall, the magnitude of ^{137}Cs, which resulted from the nuclear weapons testing, matched the range of that found by Cox & Fankhauser (1984).

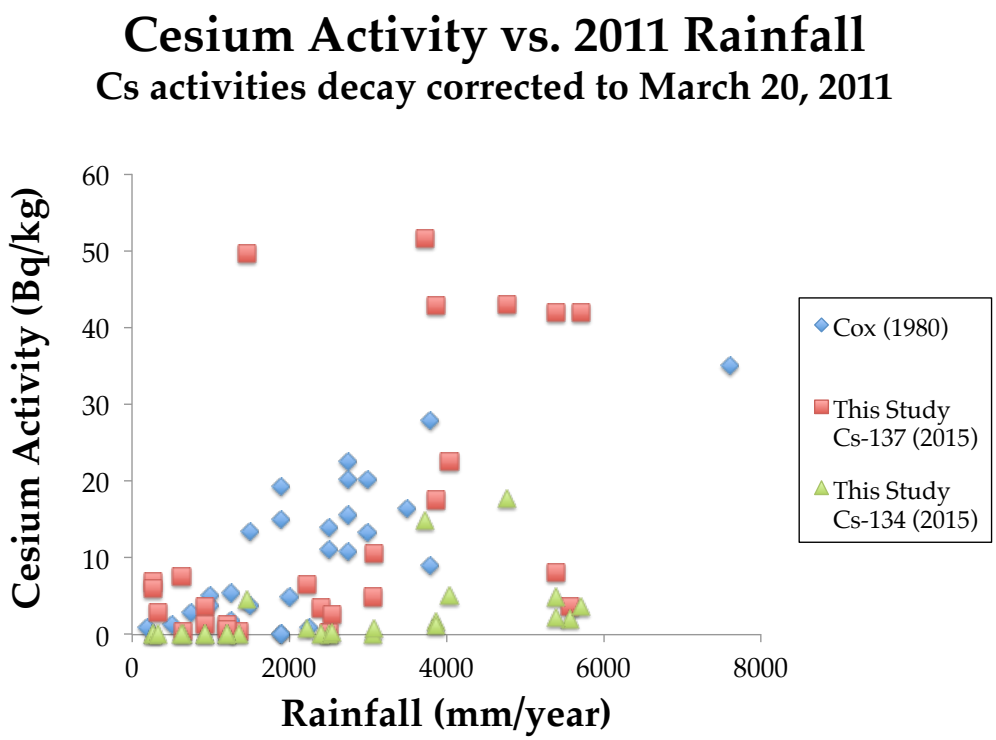

Figure 4.4.1: A comparison of measured radiocesium (Bq/kg) from Cox & Fankhauser, 1984, radiocesium measured in this study, and yearly rainfall (mm). All activities have been decay corrected to March 2011.

4.5. Natural radioisotope activities in soils

Several naturally-occurring radionuclides were used to confirm various aspects of our methodology, including the process of wet deposition, and confirmation that our soil samples were not otherwise influenced by other sources such as groundwater flow and redox chemistry.

^{7}Be is a naturally occurring radioisotope that is produced by electron capture in the upper atmosphere ($t_{1/2}$= 53.24 days) and is primarily deposited by means of precipitation (Sanders, et al., 2011). Figure 4.5.1

illustrates measured ^{7}Be activities plotted against precipitation for the month of sample collection. ^{7}Be exhibits a positive trend with precipitation, confirming that wet deposition is a major source of ^{7}Be in soils.

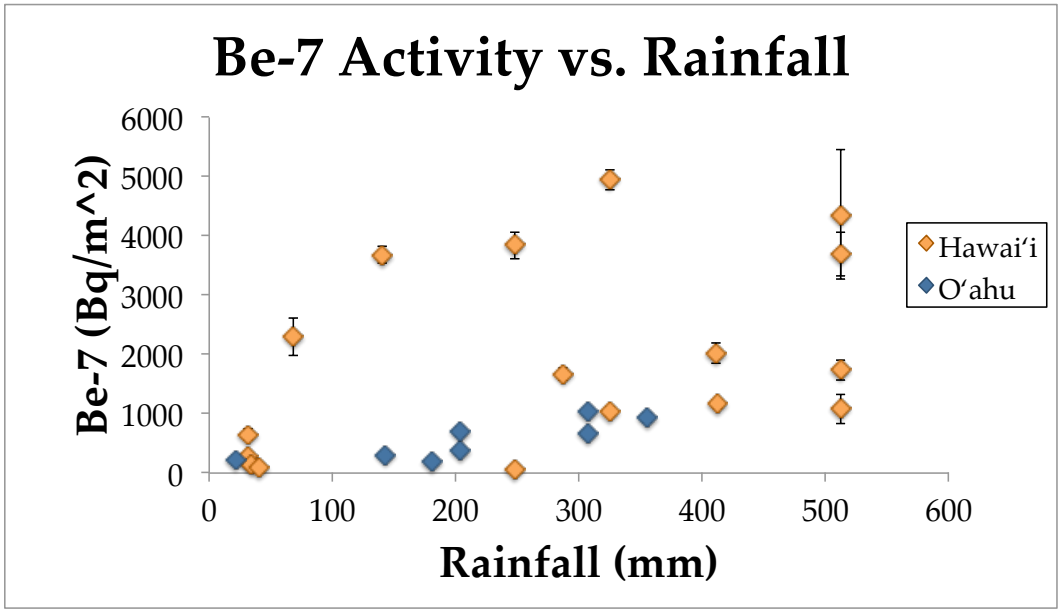

Figure 4.5.1: ^{7}Be ($t_{1/2}$= 53.24 days) activity (Bq/m^2) in soils vs. rainfall (mm) for the month of sample collection.

Similar to ^{7}Be, ^{210}Pb is a naturally occurring isotope that is primarily deposited by means of precipitation (Sanders, et al., 2011). ^{137}Cs activities and excess ^{210}Pb activities were very well correlated as shown in Figure 4.5.2. This is because they both persist long-term ($T_{1/2}$ for ^{137}Cs is about 30 years and $T_{1/2}$ for ^{210}Pb is about 20 years), they are particle reactive, and their source is atmospheric deposition. The relationship observed between ^{210}Pb and ^{137}Cs suggests that canopy cover affects ^{210}Pb deposition in a similar manner to ^{137}Cs, where the forest canopy can obstruct fallout from reaching the ground.

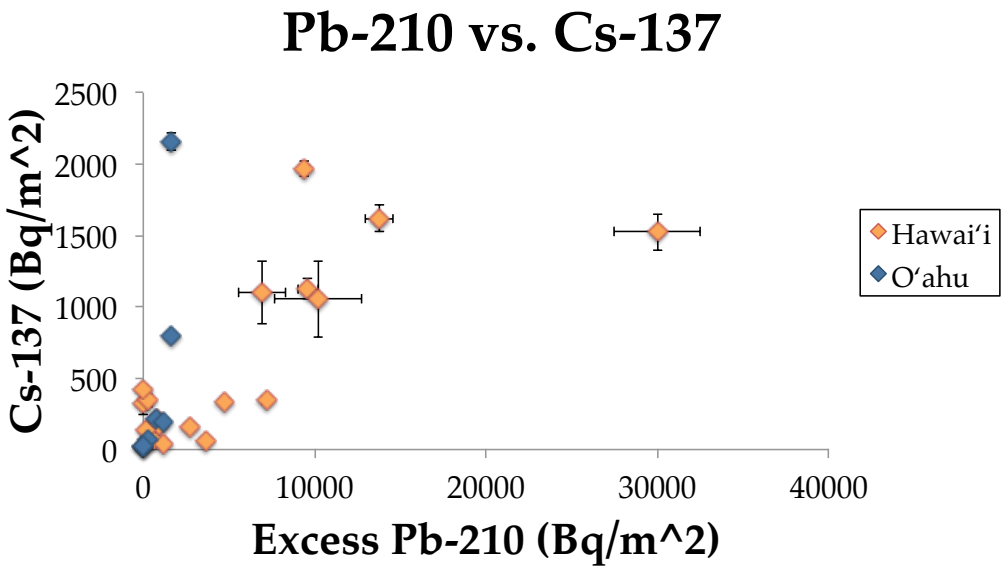

Figure 4.5.2. Excess ^{210}Pb activity in Bq/m^2 vs. ^{137}Cs activity in Bq/m^2 in soils.

^{7}Be and ^{137}Cs activities were not well correlated shown in Figure 4.5.3. These isotope activities are representative of their deposition date, which differ between one another. ^{7}Be is representative of only the three-month period prior to sample collection due to its shorter half-life and therefore reflects deposition in 2015 only. A closer relationship (Figure 4.5.4) was found comparing ^{134}Cs to ^{7}Be activities as most soil samples were collected during the same season as the Fukushima-derived deposition. ^{137}Cs inventories represent the time period of 1960 to 2015. As such, a closer relationship of ^{137}Cs with ^{210}Pb rather than ^{7}Be is not surprising.

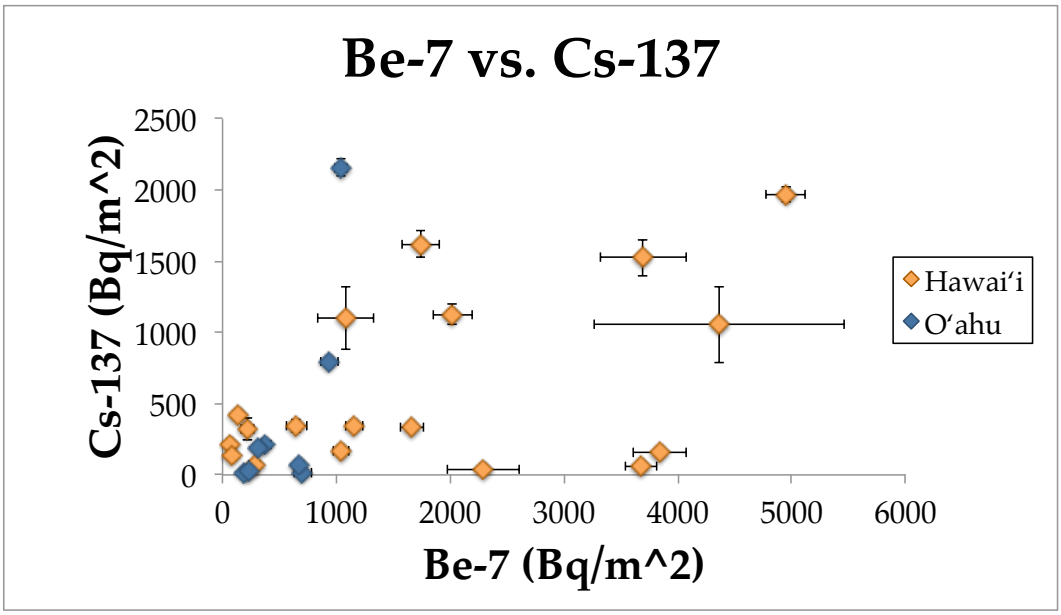

Figure 4.5.3. ^{7}Be activity in Bq/m^2 versus ^{137}Cs activity in Bq/m^2 in soils.

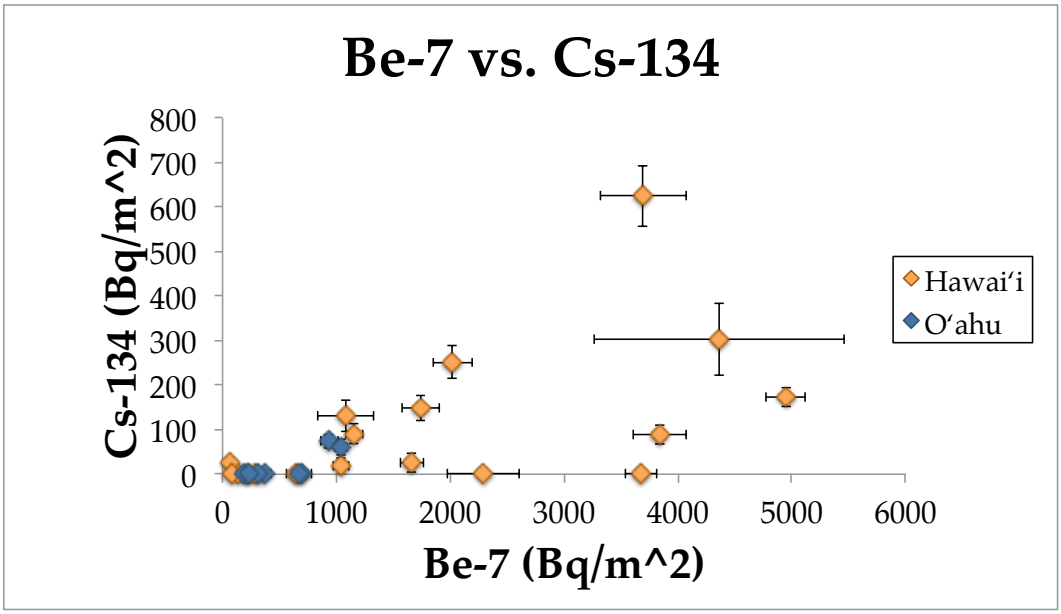

Figure 4.5.4. ^{7}Be activity in Bq/m^2 versus ^{134}Cs activity in Bq/m^2 in soils.

Soil samples on O'ahu and Hawai'i showed ^{238}U and ^{226}Ra at a near one to one ratio, as shown in Figure 4.5.5. ^{226}Ra is more mobile in groundwater that has been influenced by sources of contamination such as agriculture. Furthermore, ^{238}U tends to be mobile in oxidizing conditions and immobile in reducing conditions (Siegel, 1989). Because ^{238}U and ^{226}Ra were nearly one to one, the soils were not subject to disruption from groundwater, confirming samples were not subject to other potential sources of contamination or cesium mobilization.

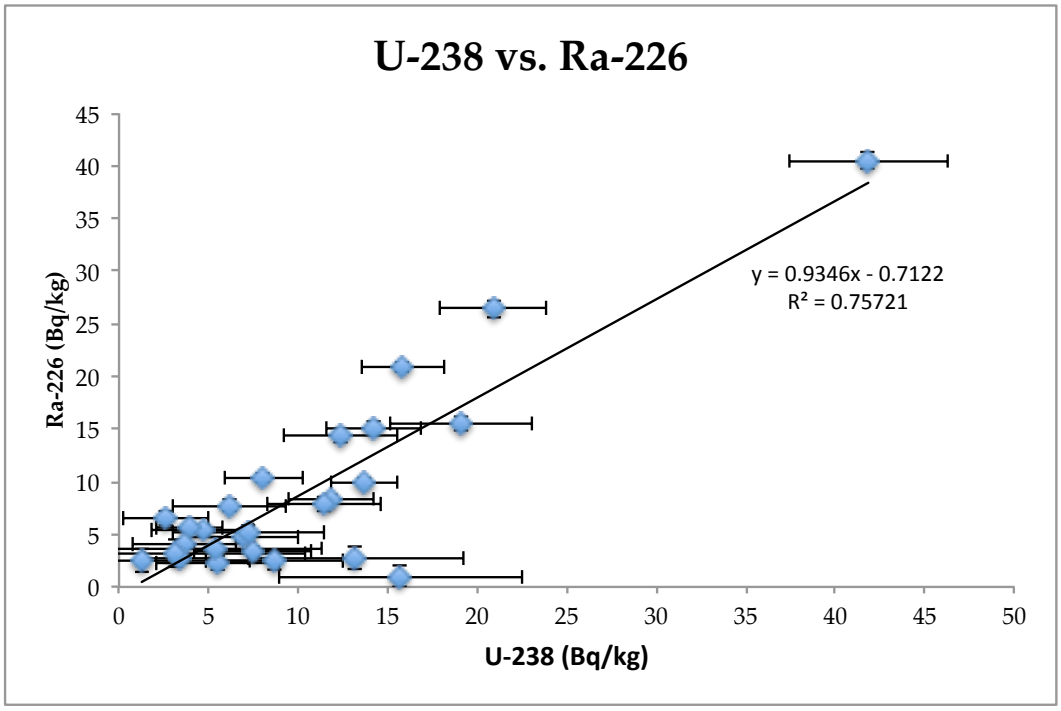

Figure 4.5.5. ^{238}U vs. ^{226}Ra activities (Bq/kg) for soils.

4.6. Comparison to previous research on fallout over the Pacific Ocean

Hawai'i is subject to unique rainfall patterns given its position, topography, and size within the Pacific Ocean. As such, we wanted to compare previous analysis of fallout by Tsumune, et al., 2003 over the Pacific Ocean to fallout in Hawai'i, while recognizing that oceanic deposition should be significantly less than the fallout found on Hawai'i because the ocean fallout values are averages and because the orografic event related to the topography of the islands. Figure 4.6.1 shows the modified time series from Tsumune, et al., 2003 comparing oceanic ^{137}Cs fallout to ^{137}Cs fallout over Hawai'i quantified in this study and decay corrected to March 20, 2011.

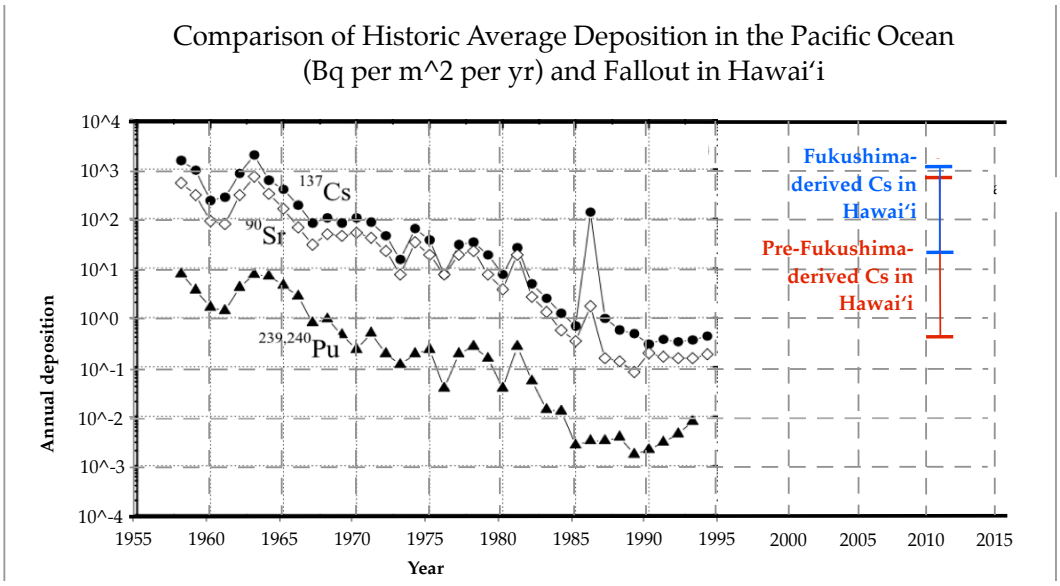

Figure 4.6.1. After Tsumune, et al., 2003. Comparison of ^{137}Cs fallout in Bq/m^2/year in the Pacific Ocean to range of ^{137}Cs fallout in Hawai'i with time.

At the same time, our data cannot allow for extrapolation over the entire Pacific Ocean. Our data strictly represents Hawaiʻi rainfall and topography and as such cannot represent oceanic deposition. The data shows that fallout on Hawaiʻi is indeed comparable to estimates by Tsumune, et al., 2003. Hawaiʻi historic fallout was derived as total pre-Fukushima inventory accumulated per 25 years and Fukushima inventory accumulated in on an impulse assumed as per year. The results show ^{137}Cs inventories measured on Hawaiʻi are similar in magnitude and range to historical ^{137}Cs fallout over the ocean.

4.7. Contemplations on Potential Health Effects

Given the study linking the Fukushima disaster to the increase of newborns born with thyroid disorders in Hawaiʻi (Mangano and Sherman, 2013), we wanted to estimate soil to milk cesium and ^{131}I transfer factors in order to investigate potential health effects. Using the levels of radiocesium and ^{131}I detected in milk samples in Hilo (DOH, 2011) and our measured Fukushima-derived cesium inventories and inferred ^{131}I inventories from the Hilo area, we estimated the soil to milk transfer factors. Based on these transfer factors, soils in the Hilo area would have to be about 1200 times more enriched in cesium and 260 times more enriched in ^{131}I in order for milk on the island of Hawaiʻi to reach the derived intervention limit. Derived intervention limits are determined with concern to human health and as such measured cesium inventories and inferred ^{131}I inventories are significantly below these levels and thus the study on increase in thyroid disorders in Hawaiʻi is questionable.

CHAPTER 5. CONCLUSION

The presence of Fukushima-derived fallout in mushrooms and soils on Oʻahu has been confirmed. The level of radioactivity detected, however, is many magnitudes lower than a level of health concern. Mushrooms proved useful indicators of fallout locations, but soil samples were necessary to quantify the deposited amount. Cesium activity between soil and mushrooms were not well correlated. This is due to the difference in bioaccumulation rates between mushroom species. Furthermore, higher rainfall in March 2011 resulted in elevated Fukushima-derived cesium in both mushrooms and soil. Fukushima-derived cesium, however, was not detectable in basalt samples and the overall cesium inventory in these samples was very low. All soil samples with detectable Fukushima-derived cesium were classified as deficient in potassium, acidic, and as having a high to very high water holding capacity by the Hawaiʻi Soil Atlas. The lack of canopy cover seemed to be an important factor in Fukushima-derived cesium deposition. Consistent with previous analysis by Cox & Fankhauser in 1984, rainfall above 300 mm/month or 3600 mm/year resulted in elevated cesium deposition. Moreover, Fukushima-derived cesium levels were an order of magnitude lower than those from nuclear weapons fallout measured by Cox & Fankhauser in 1980's.

BIBLIOGRAPHY

Buesseler, K., Aoyama, M., & Fukasawa, M. (2011). Impacts of the Fukushima Nuclear Power Plants on Marine Radioactivity. Environmental Science & Technology Environ. Sci. Technol., 45(23), 9931-9935.

Castro, L. D., Maihara, V., Silva, P., & Figueira, R. (2012). Artificial and natural radioactivity in edible mushrooms from Sao Paulo, Brazil. Journal of Environmental Radioactivity, 113, 150-154.

Cox, M. E., & Fankhauser, B. L. (1984). Distribution of Fallout Cesium-137 in Hawaii. Health Physics, 46(1), 65-71.

Department of Health (DOH) (2011). Milk Sample Shows Trace Amounts of Radiation in Milk from Big Island Dairy.

Duff, M.C., & Ramsey M.L. (2008). Accumulation of radiocesium by mushrooms in the environment: a literature review. Journal of Environmental Radioactivity, 99(6): 912-23, doi:10.1016/j.jenvrad.2007.11.017

Environmental Protection Agency (EPA) (2011). RADNET Database.

Filipović-Vinceković, N., Barišić, D., Mašić, N., & Lulić, S. (1991). Distribution of fallout radionuclides through soil surface layer. Journal of Radioanalytical and Nuclear Chemistry, Articles Journal of Radioanalytical and Nuclear Chemistry Articles, 148(1), 53-62.

Fujii, K., Ikeda, S., Akama, A., Komatsu, M., Takahashi, M., & Kaneko, S. (2014). Vertical migration of radiocesium and clay mineral composition in five forest soils contaminated by the Fukushima nuclear accident. Soil Science and Plant Nutrition, 60(6), 751-764. doi:10.1080/00380768.2014.926781

Giambelluca, T.W., Q. Chen, A.G. Frazier, J.P. Price, Y.-L. Chen, P.-S. Chu, J.K. Eischeid, and D.M. Delparte, 2013: Online Rainfall Atlas of Hawai‘i. *Bull. Amer. Meteor. Soc.* 94, 313-316, doi: 10.1175/BAMS-D-11-00228.1.

Hawaii Soil Atlas. (2014). http://gis.ctahr.hawaii.edu/SoilAtlas

Kaduka, M., Shutov, V., Bruk, G., Balonov, M., Brown, J., & Strand, P. (2006). Soil-dependent uptake of 137Cs by mushrooms: Experimental study in the Chernobyl accident areas. Journal of Environmental Radioactivity, 89(3), 199-211.

Kato, H. Onda, Y., and Teramage M. (2012). Depth distribution of 137Cs, 134Cs, and 131I in soil profile after Fukushima Dai-ichi Nuclear Power Plant Accident. Journal of Environmental Radioactivity, 111, 59-64.

Mangano, J. J., & Sherman, J. D. (2013). Elevated airborne beta levels in Pacific/West Coast US States and trends in hypothyroidism among newborns after the Fukushima nuclear meltdown. OJPed Open Journal of Pediatrics, 03(01), 1-9.

Nakashima, K., Orita, M., Fukuda, N., Taira, Y., Hayashida, N., Matsuda, N., & Takamura, N. (2015). Radiocesium concentrations in wild mushrooms collected in Kawauchi Village after the accident at the Fukushima Daiichi Nuclear Power Plant. PeerJ, 3.

Oolbekkink, G. T., & Kuyper, T. W. (1989). Radioactive caesium from Chernobyl in fungi. *Mycologist, 3*(1), 3-6.

Pararas-Carayannis, G. (2013). The Great Tohoku-Oki Earthquake and Tsunami of March 11, 2011 in Japan: A Critical Review and Evaluation of the Tsunami Source Mechanism. Pure and Applied Geophysics Pure Appl. Geophys., 171(12), 3257-3278.

Révay, Zs., Belgya,T., Ember, P. P. , Molnár, G. L..(2001). Recent Developments in HYPERMET PC, Journal of Radioanalytical Nuclear Chemistry, 248,401-405.

Ritchie, J. C., & Mchenry, J. R. (1990). Application of Radioactive Fallout Cesium-137 for Measuring Soil Erosion and Sediment Accumulation Rates and Patterns: A Review. Journal of Environment Quality, 19(2), 215.

Sanders, C. J., Smoak, J. M., Cable, P. H., Patchineelam, S. R., & Sanders, L. M. (2011). Lead-210 and Beryllium-7 fallout rates on the southeastern coast of Brazil. Journal of Environmental Radioactivity, 102(12), 1122-1125.

Seeger, R. (1978). Potassium Content Of Wild Mushrooms. Abstracts, 583.

Siegel, D. I. (1989). Geochemistry of the Cambrian-Ordovician aquifer system in the northern Midwest, United States, 40-42.

Tanaka, S., & Kado, S. (2014). Analysis of Radioactive Release from the Fukushima Daiichi Nuclear Power Station. Reflections on the Fukushima Daiichi Nuclear Accident, 51-83.

Teramage, M. T., Onda, Y., & Kato, H. (2016). Small scale temporal distribution of radiocesium in undisturbed coniferous forest soil:

Radiocesium depth distribution profiles. Journal of Environmental Management, 170, 97-104.

Thakur, P., Ballard, S., & Nelson, R. (2013). An overview of Fukushima radionuclides measured in the northern hemisphere. Science of The Total Environment, 458-460, 577-613.

Tsumune, D., Aoyama, M., Hirose, K. (2003). Behavior of 137 Cs concentrations in the North Pacific in an ocean general circulation model. J. Geophys. Res. Journal of Geophysical Research, 108(C8).

United Nations Scientific Committee on the Effects of Atomic Radiation. Sources and effects of ionizing radiation. United Nations Scientific Committee on the Effects of Atomic Radiation 2000 report to the general assembly with scientific annexes. New York: United Nations; Publication E 00:IX.3; 2000.

Wetherbee, G. A., Gay, D. A., Debey, T. M., Lehmann, C. M., & Nilles, M. A. (2012). Wet Deposition of Fission-Product Isotopes to North America from the Fukushima Dai-ichi Incident, March 2011. Environmental Science & Technology Environ. Sci. Technol., 46(5), 2574-2582.